8-2010

Synthesis, Kinetic and Photocatalytic Studies of Porphyrin-Ruthenium-Oxo Complexes

Yan Huang
Western Kentucky University, yan.huang607@wku.edu

SYNTHESIS, KINETIC AND PHOTOCATALYTIC STUDIES OF PORPHYRIN-RUTHENIUM-OXO COMPLEXES

A Thesis

Presented to

The Faculty of the Department of Chemistry

Western Kentucky University

Bowling Green, Kentucky

In Partial Fulfillment

Of the Requirements for the Degree

Master of Science in Chemistry
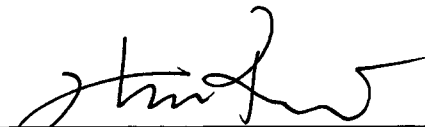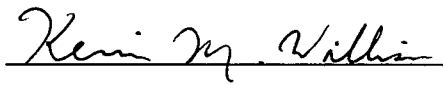
By

Yan Huang

August 2010

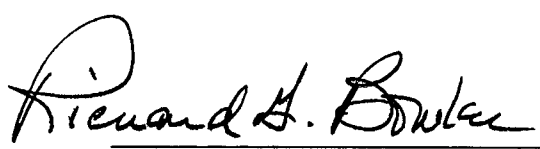# SYNTHESIS, KINETIC AND PHOTOCATALYTIC STUDIES OF PORPHYRIN-RUTHENIUM-OXO COMPLEXES

Date Recommended ___7/14/2010___

_____
Director of Thesis

_____

_____

_____
Dean, Graduate Studies and Research   Date

TABLE OF CONTENTS

LIST OF TABLES

LIST OF FIGURES

v

LIST OF SCHEMES

ABBREVIATIONS AND SYMBOLS

Ar-H	Aryl hydrogen
β-H	Pyrrolic hydrogen
$BF_3 \cdot OEt_2$	Boron trifluoride diethyl etherate
CYP450	Cytochrome P450
$CYP450_{cam}$	Cytochrome $P450_{cam}$
DDQ	2,3-Dichloro-5,6-dicyano-p-benzequinone
DMF	N,N-Dimethylformamide
FID	Flame ionization detector
FT-IR	Fourier-transform infrared
GC	Gas chromatograph
$H_2(F_{20}$-tpp)	5,10,15,20-tetrakis(pentafluorophenyl)porphyrin
^{1}H-NMR	Proton nuclear magnetic resonance
H_2TMP	*meso*-tetramesitylporphyrin
H_2TMPyP	5,10,15,20-tetrakis(1-methyl-4-pyridinio)porphyrintetra(p-toluenesulfonate)
H_2TPFPP	*meso*-tetrakis(5,10,15,20-pentafluorophenyl)porphyrin
H_2TPP	*meso*-tetraphenylporphyrin
KIE	Kinetic isotope effect
k_0	Background rate constant
k_2	Second-order rate constant
k_{obs}	Observed pseudo-first-order rate constant

k_{rel}	Relative rate constant
m-CPBA	*meta*-Chloroperoxybenzoic acid
NADH	Nicotinamide adenine dinucleotide
NADPH	Nicotinamide adenine dinucleotide phosphate
PhIO	Iodosylbenzene
[Ru^{II}(CO)(4-CF$_3$-TPP)]	
	Carbonyl[4-trifluoromethyl-(5,10,15,20-tetraphenylporphyrinato)] ruthenium(II)
[Ru^{II}(CO)TMP]	Carbonyl(5,10,15,20-tetramesitylporphyrinato)ruthenium(II)
[Ru^{II}(CO)TPFPP]	Carbonyl[5,10,15,20-tetrakis(pentafluorophenyl)porphyrinato] ruthenium(II)
[Ru^{IV}(4-CF$_3$-TPP)(OH)]$_2$O	
	μ-oxo-bis[(hydroxo)(4-trifluoromethyl-(5,10,15,20-tetraphenylporphyrinato)) ruthenium(IV)]
[Ru^{VI}(O)$_2$TMP]	*trans*-dioxo(5,10,15,20-tetramesitylporphyrinato) ruthenium(VI)
[Ru^{VI}(O)$_2$TPP]	*trans*-dioxo(5,10,15,20-tetraphenylporphyrinato) ruthenium(VI)
[Ru^{VI}(O)$_2$TPFPP]	*trans*-dioxo[5,10,15,20-tetrakis(pentafluorophenyl)porphyrinato] ruthenium(VI)
TBHP	*tert*-Butyl hydroperoxide
TON	Turnover number
UV-vis	Ultraviolet-visible

ACKNOWLEDGEMENT

SYNTHESIS, KINETIC AND PHOTOCATALYTIC STUDIES OF PORPHYRIN-RUTHENIUM-OXO COMPLEXES

Yan Huang   August 2010   80 Pages

Directed by: Dr. Rui Zhang

Department of Chemistry   Western Kentucky University

Macrocyclic ligand-complexed transition metal-oxo intermediates are the active oxidizing species in a variety of important biological and catalytic oxidation reactions. Many transition metal catalysts have been designed to mimic the predominant oxidation catalysts in Nature, namely the cytochrome P450 enzymes. Ruthenium porphyrin complexes have been the center of the research and have successfully been utilized, as catalysts, in major oxidation reactions such as the hydroxylation of alkanes. This study focuses on kinetic and photocatalytic studies of oxidation reactions with well-characterized high-valent ruthenium-oxo porphyrin complexes.

The *trans*-dioxoruthenium(VI) porphyrins have been among the best-characterized metal-oxo intermediates and their involvement as the active oxidant in the hydrocarbon oxidation have been extensively studied. Following the literature known methods, a series of *trans*-dioxoruthenium(VI) porphyrin complexes (**3a-b**) were synthesized and spectroscopically characterized by UV-vis, IR and ^{1}H-NMR. In addition to the well-known chemical methods, we developed a novel photochemical approach for generation of *trans*-dioxoruthenium(VI) porphyrins with visible light. The fast kinetic study of two-electron oxidations of *para*-substituted phenyl methyl sulfides by these

dioxoruthenium(VI) species was conducted by using stopped-flow spectroscopy. Results showed that the decay of *trans*-dioxoruthenium(VI) porphyrins in the presence of reactive sulfides follows a biexponential process. The reactivity order in the series of dioxoruthenium complexes follows TPFPP>TPP>TMP, consistent with expectations based on the electrophilic nature of high-valent metal-oxo species. Moreover, the sulfoxidation reactions are 3 to 4 orders of magnitude faster than the well-known epoxidation reactions. In addition, several ruthenium porphyrins were used as the catalysts in the competitive oxidation reactions to identify the kinetically competent oxidants during catalytic turnover conditions.

The photocatalytic studies of aerobic oxidation reactions of hydrocarbons catalyzed by a bis-porphyrin-ruthenium(IV) μ-oxo dimer using atmospheric oxygen as oxygen source in the absence of co-reductants were investigated as well. The ruthenium(IV) μ-oxo bisporphyrin (**6a**) was found to catalyze aerobic oxidation of a variety of organic substrates efficiently. By comparison, **6a** was found to be more efficient photocatalyst than the well-known **3a** under identical conditions. A KIE at 298K was found to be larger than those observed in autoxidation processes, suggesting a nonradical mechanism that involved the intermediacy of ruthenium(V)-oxo species as postulated.

I. INTRODUCTION

1.1. <u>General</u>

Catalytic oxidation is one of the most important technologies for the production of commodity chemicals, and the key to fundamental transformations in Nature as well.[1] To date, most of the oxidation reactions have been performed with relatively expensive reagents that generate heavy-metal waste, and are usually run in environmentally undesirable solvent, typically chlorinated hydrocarbons.[2] The development of new processes that employ transition metals as substrate-selective catalysts and a stoichiometric environmentally friendly oxygen source, such as molecular oxygen or hydrogen peroxide, is one of the most significant goals in oxidation chemistry.[1] Those oxidants are atom efficient and produce water as the only by-product, are becoming more important in fine chemical manufacturing.[2]

In biological system, catalytic oxidations mediated by oxidative enzymes form the basis of a great many biosynthetic and biodegradative processes.[3] According to early works reported by Hayaishi and co-workers, Nature has found many ways to utilize atmospheric dioxygen to functionalize molecules through the use of a diverse set of cofactors.[4] Flavin, non-heme iron, copper, and metalloporphyrin complexes have all been conscripted to metabolize atmospheric dioxygen in an oxygenase catalytic cycle, resulting in the incorporation of one or both oxygen atoms into the substrate.[4] This study is inspired by one of the heme-containing enzymes, termed cytochrome P450s (abbreviated as CYP). Although members are of the large group of oxygenases, the cytochrome P450s play a variety of critical roles in biology.

Many members of the cytochrome P450 superfamily of hemoproteins are currently known, and the numbers continue to grow as more genomes are sequenced. To date, over 8100 distinct cytochrome P450 genomes are known to exist, but few have been studied in detail. The cytochrome P450s have been found in all branches of the "tree of life" that catalogs the diversity of life forms, including plants, bacteria, fungi, insects, human beings and so on. Moreover, they can be isolated in numerous mammalian tissues as well, like liver, kidney, lung, and intestine.[4] In the broadest terms, there are two main functional roles for these oxygenses. One is the metabolism of drugs and xenobiotics (compounds exogenous to the organism) as a protective role of degradation in preparation for excretion. A second broad functional role is in the biosynthesis of critical signaling molecules used for control of development and homeostasis. In mammalian tissues the P450s play these roles through the metabolism of drugs and xenobiotics, the synthesis of steroid hormones and fat-soluble vitamin metabolism, and the conversion of polyunsaturated fatty acids to biologically active molecules, respectively.[4]

The important metabolic role together with the unique chemistry and physical properties of the cytochrome P450s provides a strong attraction for scientists in many disciplines.[4] Relevance to human health is the initial focus of pharmacologists and toxicologists. The role of metal centers and their associated unique spectral properties in the cytochrome P450s is a magnet for bioinorganic chemists and biophysicists.[5] The difficult conversion of unactivated hydrocarbons attracted the bioorganic chemist.[5] A continuing challenge is to understand how the diverse set of substrate specificities and metabolic transformations are determined by the precise nature of the heme-iron oxygen and protein structure. The structure and electronic configuration of the "active oxygen"

intermediates which serve as efficient catalysts remains an area of active research.[4] The

most common heme prosthetic group found in heme-containing enzymes is the iron

protoporphyrin IX (heme *b*) complex,[5] which is reported as the active site of the heme

enzymes (Figure 1).[3]
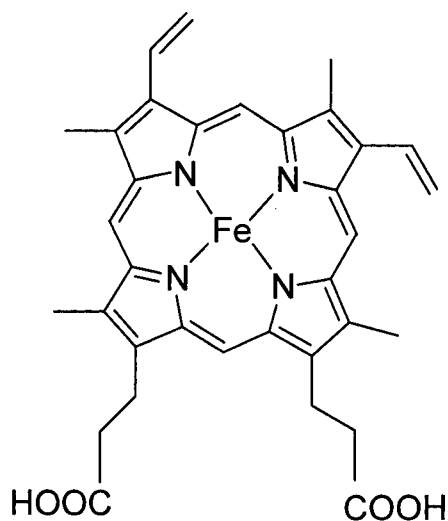
Figure 1. Structure of iron protoporphyrin IX (Heme *b*)

Cytochrome P450 enzymes can be further classified into two categories,

monooxygenases and dioxygenases, depending on whether one or both oxygen atoms

from dioxygen are incorporated into substrate (Schemes 1 and 2),[5]

$$XH \ + \ {}^*O_2 \ \longrightarrow \ X({}^*O_2)H$$
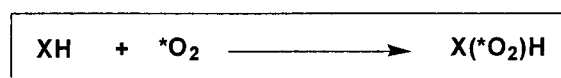
Scheme 1. Monooxygenase reaction

$$XH \ + \ {}^*O_2 \ + \ AH_2 \ \longrightarrow \ X({}^*O)H \ + \ H_2{}^*O \ + \ A$$
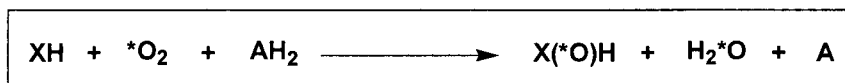
Scheme 2. Dioxygenase reaction

Where XH and AH_2 represent substrate and an electron donor, respectively.[5] Monooxygenases require two electrons to reduce the second oxygen atom of dioxygen to water (Scheme 1). Cytochrome P450 has benefited from the attention of inorganic, organic, and physical chemists since its discovery due to its unique spectral properties as well as its ability to efficiently catalyze a variety of difficult biotransformations.[5] Many of the heme-containing oxygenases go through a ferrous-dioxygen complex as a key intermediate in their catalytic reaction cycles. Moreover, P450 is able to utilize either NADH or NADPH as the electron donor in catalyzing monooxygenation reactions.[5] The two electrons can come from a reducing agent like NADH (external monooxygenase) or from the substrate itself (internal monooxygenase). Similarly, dioxygenases are subcategorized into intermolecular and intramolecular classifications depending on whether the two oxygen atoms are incorporated into separate substrates or into a single molecule. Clearly, the terms mono- and dioxygenase relate only to the stoichiometry of the oxygen incorporation reaction and not to the mechanism of dioxygen activation.[5,6]

The name cytochrome P450 arises from the fact that the reduced protein efficiently binds carbon monoxide with a strong absorption band (the Soret $\pi - \pi^*$ band) at 450 nm. This spectroscopic property has been very useful in the early studies on cytochromes P450 to monitor the presence of this enzyme in the microsomal fraction of liver tissues.[7,8] With the exception of microbial P450s, the majority of P450 enzymes are membrane-bound, being associated with either the inner mitochondrial or the endoplasmic reticulum (microsomal) membranes. In fact, the majority of the physiological substrates such as steroids and fatty acids as well as xenobiotic molecules are highly hydrophobic. A soluble, camphor-inducible, bacterial P450 monooxygenase

(P450 CAM) system was discovered in *Pseudomonas putida* by Gunsalus and co-workers.[5] Being soluble, it was quickly possible to purify this P450 enzyme in large quantity. Cytochrome P450 is no longer a black box since Poulos et al. provided the first tri-dimensional structure of the cytochrome $P450_{cam}$ (Figure 2) in 1986, which catalyzes the stereospecific hydroxylation of the exo C_5-H bond of camphor (Scheme 3).[7]

Figure 2. X-ray structure of cytochrome $P450_{cam}$
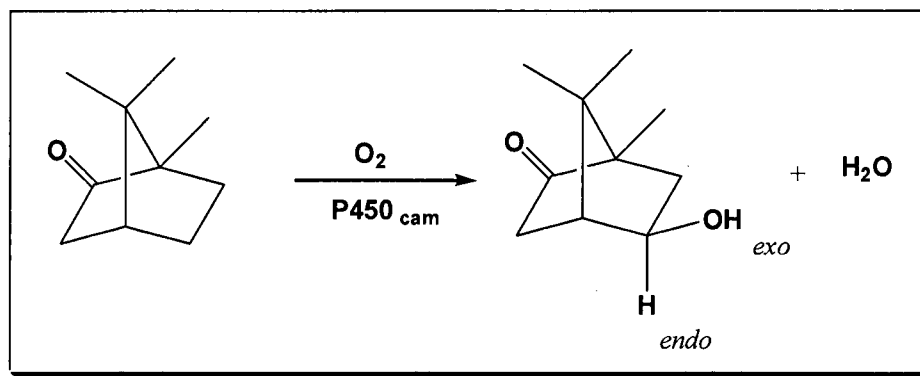
Scheme 3. Stereospecific hydroxylation of the exo C-H bond at position 5 of camphor by cytochrome P450$_{cam}$

More than 50 years after the discovery of cytochrome P450 enzymes, the exact nature of the active species (the putative high-valent iron-oxo intermediate) is still a matter of intensive debates.[7] However, the oxidant in a P450 enzyme is usually thought to be an iron(IV)-oxo porphyrin radical cation, termed Compound I, by analogy to the intermediates formed in peroxidase and catalase enzymes.[9] With the development of the new processes, iron, manganese, and ruthenium transition metals have been employed as substrate-selective catalysts of biomimic models of the cytochrome P450 enzymes.[7] In the past decades, many synthetic metalloporphyrin complexes have been reported as model compounds of heme-containing enzymes and catalysts for a variety of selective oxidation reactions (Scheme 4).[7] This study was stimulated by the desire for the better understanding of the intricate mechanisms of biochemical oxidations using simple biomimetic models.
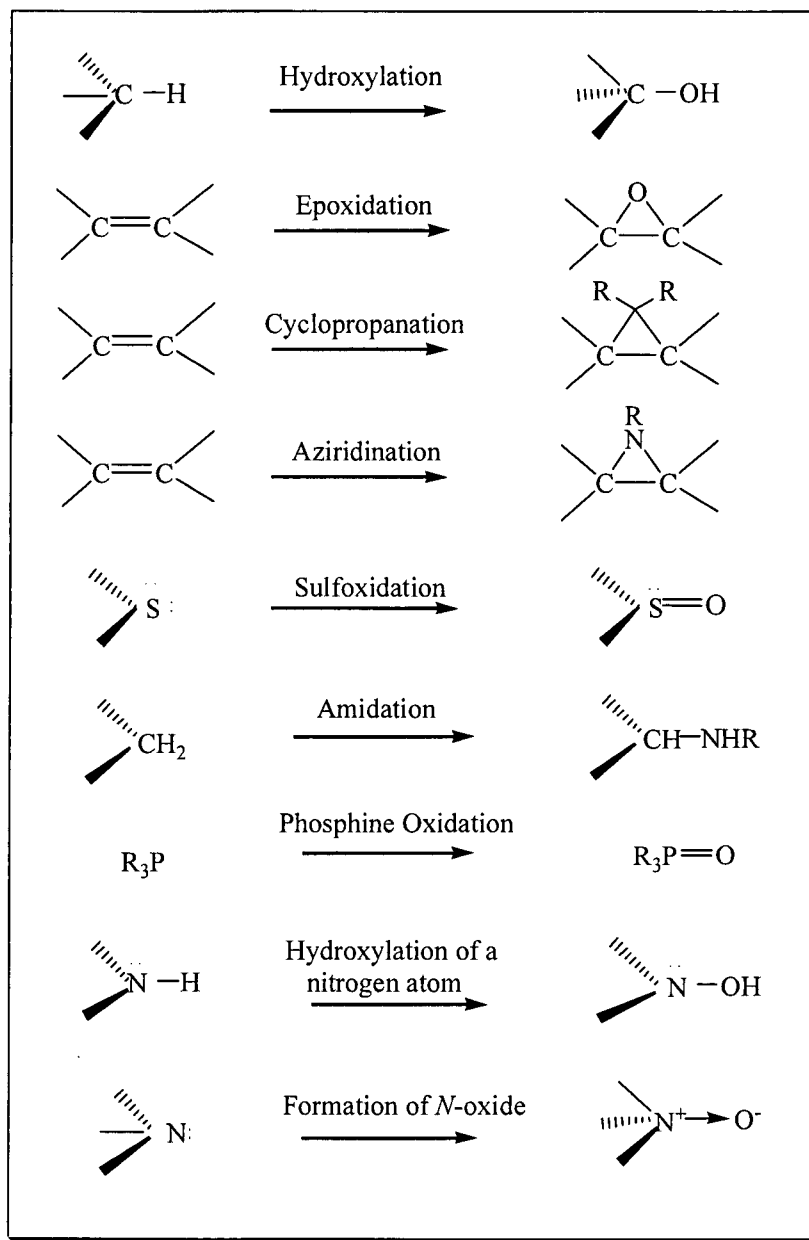
Scheme 4. Typical metalloporphyrin-mediated reactions

In this work, a series of ruthenium porphyrin complexes have been synthesized and characterized. The study focuses on kinetic studies of the sulfoxidation of aryl methylsulfides by *trans*-dioxoruthenium(VI) porphyrin complexes and photocatalytic aerobic oxidation by a bis-porphyrin-ruthenium(IV) μ-oxo dimer.

1.2. Biomimetics Models of Cytochrome P450 Enzymes

The controlled oxygenation of alkanes and alkenes is one of the most important technologies for the conversion of petroleum products to valuable commodity chemicals.[10] Many of these processes utilize metal catalysts to promote both the rate of reaction and product selectivity. There is considerable pressure to replace old technologies with more efficient alternatives using dioxygen, hydrogen peroxide or other easily accessible and environmentally friendly oxidants.[11,12] Nature selected iron porphyrins to mediate intrinsically difficult oxidations with dioxygen at the heme center of cytochrome P450 monooxygenases.[13] Effective catalytic systems for hydrocarbon oxidation based on metalloporphyrin catalysts with iron, manganese and ruthenium complexes have been received current attentions. A variety of cytochrome P450 models has been developed over the past decades and applied to hydrocarbon oxidations with the aims of both developing useful catalysts and probing the mechanisms of these processes.[14]

High-valent oxo metalloporphyrins have been known as reactive intermediates in the catalytic cycles of many heme enzymes and in the oxidation reactions mediated by synthetic metalloporphyrins.[7,10] Studies using synthetic metalloporphyrins as models for cytochrome P450 have afforded important insights into the nature of the enzymatic processes.[14,15] The first high-valent iron-oxo porphyrin complex has been isolated by Groves et al. by oxidation of $Fe^{III}(Cl)TMP$ with m-chloroperbenzoic acid at low temperature.[7] Iron(IV)-oxo porphyrin radical cations are observed intermediates in peroxidase and catalase enzymes, where they are known as Compound I species.[5] Although not detected under turnover conditions, a Compound I species is also thought to

be an active oxidant in the cytochrome P450 enzymes (P450s).[16,17] Until 2007, according to works reported by Collins and co-workers, iron(V)-oxo species have been proposed as key reactive intermediates in the catalysis of oxygen-activating enzymes and synthetic catalysts.[18] In this report, mass spectrometry, electron paramagnetic resonance, and x-ray absorption spectroscopies, as well as reactivity studies and density functional theory calculations demonstrate this long-lived (hours at -60 °C) intermediate is a spin S=1/2 iron(V)-oxo complex.[18]

Besides iron-oxo porphyrin complex, the chemistry of high-valent ruthenium-oxo and manganese-oxo intermediates have received considerable attention.[14] Manganese porphyrins have been shown to have unusually high reactivity toward olefin epoxidation and alkane hydroxylation.[14] For instance, the reaction of the water-soluble tetra-*N*-methyl-4-pyridylporphyrinatomanganese(III) [Mn^{III}(TMPyP)] with a variety of oxidants was first reported by Meunier and co-workers to produce a manganese-oxo intermediate which underwent rapid oxo–aqua interconversion.[10] Recently, the detection of an oxomanganese(V) porphyrin intermediate under ambient conditions by using rapid mixing stopped-flow techniques has allowed a direct assessment of its reactivity.[19]

Ruthenium porphyrins and related complexes attracted more attention because of the close periodic relationship to the biologically significant iron and the rich coordination and redox chemistry of ruthenium. Ruthenium has the widest scope of oxidation states from -2 to +8 in various ligand environments. Since ruthenium complexes have a variety of useful characteristics including high Lewis acidity, high electron transfer ability, low redox potentials and stability of reactive metal species, a great number of new and significant reactions have been developed by using both

stoichiometric and catalytic amounts of ruthenium complexes.[3] For example, ruthenium

porphyrin complexes such as carbonylruthenium(II) tetrakispentafluorophenylporphyrin

[Ru^{II}(CO)TPFPP] efficiently catalyzed the hydroxylation of unactivated alkanes, the

cleavage of ethers, and the oxygenation of benzene with 2,6-dichloropyridine N-oxide as

the oxidant under mild, nonacidic conditions (Scheme 5).[13]
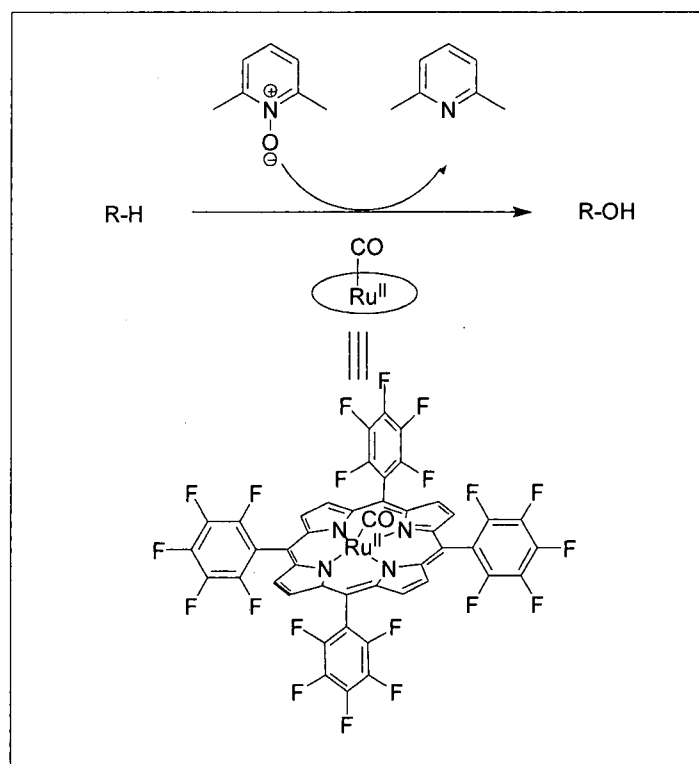
Scheme 5. Hydroxylation of hydrocarbons with 2,6-dichloropyridine N-oxide catalyzed

by Ru^{II}(CO)TPFPP

In particular, *trans*-dioxoruthenium(VI) porphyrin complexes are a significant

class of ruthenium oxidants, which are neutral and readily dissolve in nonpolar organic

solvent, and yet are reactive toward alkene epoxidations and alkane hydroxylations.

Furthermore, they also can be modified by attaching chiral auxiliaries onto the

porphyrinato ligands providing an access to highly reactive chiral metal-oxo reagents.[3] In

this work, a new photochemical method has been developed to produce *trans*-dioxoruthenium(VI) complexes that employ sterically hindered and unhindered porphyrin ligands.[20]

1.3. <u>Sulfoxidation Reactions</u>

The oxidation of sulfides to sulfoxides is of significant importance in organic chemistry, both for fundamental research and for a wide range of applications.[21] Organic sulfoxides are versatile synthons for C–C bond formation, molecular rearrangements, functional group transformations and are also utilized as precursors for biologically active and chemically important compounds.[22] The selective and catalytic oxidation of sulfur is a key reaction in organic synthesis. Thus, selective oxidation of organic sulfides is very important from both industrial and green chemistry points of view as organosulfur compounds are a major source of environmental pollution.[23] Moreover, organic sulfoxides are very valuable synthetic intermediates for the production of a range of chemically and biologically active molecules including therapeutic agents such as anti-ulcer (proton pump inhibitors), antibacterial, antifungal, anti-atherosclerotic, antihypertensive and cardiotonic agents as well as psychotropics and vasodilators.[24] The growing attention and applications of sulfoxides have stimulated research into new methods for their synthesis.

The oxidation of sulfides is the most straightforward method for the synthesis of sulfoxides.[25] There are a lot of reagents available for the oxidation of sulfides. Unfortunately, most of these reagents are not satisfactory. They are either harmful or

expensive, and a simple procedure is not easily available, because of the over-oxidation of sulfoxides to sulfones.[21] Therefore, controlling the reaction conditions, that is, time, temperature and the relative amount of oxidants, plays an important role to avoid forming over oxidation products; however, these requirements are often hard to meet. Thus, there is still considerable interest in the development of selective oxidations methods for this transformation.[24]

The synthesis of sulfoxides was first reported by Marcker in 1865 and, since then, a number of methods have been developed for the conversion of sulfides into sulfoxides.[21] Based on the reports by Kowalski and co-workers, hydrogen peroxide is considered as an ideal "green" oxidant due to its strength and lack of toxic by-products.[21] Besides, Hosseinpoor and Golchoubian reported a very efficient and selective oxidation of sulfides to the corresponding sulfoxides using H_2O_2 catalyzed by Mn(III) Schiff-base complex under mild conditions.[24] Moreover, *N*-bromosuccinimide for the oxidation of sulfides has usually been carried out using anhydrous solvents at various temperatures without any over-oxidation to sulfones.[22] Kolarska and co-workers also considered oxidizing sulfides with molecular halogens due to its low price, easy handling, commercial availability, and relatively high stability.[21]

Since hydrogen peroxide works very well as an ideal oxidant, sulfoxidation catalyzed by transition metal-oxo complexes has received less attention. Recently, extensive studies on the epoxidation and hydroxylation of hydrocarbons by *trans*-dioxoruthenium(VI) porphyrins are well established in the scientific literature.[3] However, studies on sulfoxidation reactions by the well-characterized *trans*-dioxoruthenium(VI) porphyrin complexes are still not known yet.

1.4. Photocatalytic Aerobic Oxidations

The selective oxidation of organic molecules solely by molecular oxygen is one of the holy grails in chemistry, which is also a key technology for the synthesis of high value chemicals in the pharmaceutical and petrochemical industries.[26-28] Many stoichiometric oxidants with heavy metals are expensive, toxic and impractical. Thus, the ideal green catalytic oxidation process would use molecular oxygen or hydrogen peroxide as the primary oxygen source with recyclable catalysts in nontoxic solvents. Moreover, processes that rely on metal-oxo species are usually selective. However, there is an intrinsic problem: when the reducing power of a given metal complex is sufficient to activate molecular oxygen, the oxidizing power of its higher valent form is usually not strong enough to oxidize organic substrates.[29] One of solutions is to use 4d and 5d metals that have a larger number of accessible oxidation states. One of the most outstanding examples is a catalytic aerobic oxidation driven by a photodisproportionation reaction employed a diiron(III)-μ-oxo bisporphyrin complex with no added reducing agent.[30] The limitation by using iron porphyrins as practical photocatalysts is the low reactivity of the formed iron(V)-oxo transients and poor quantum efficiency, but the catalytic efficiency of diiron(III)-μ-oxo bisporphyrin systems was improved by Nocera and co-workers who employed "Pacman" ligand (Scheme 6).[31] Photocatalytic oxidation cycles using Pacman systems have been turned over with easily oxidized organic substrates and, more recently, with olefins by using electron-deficient diiron(III)-μ-oxo bisporphyrins.[32]
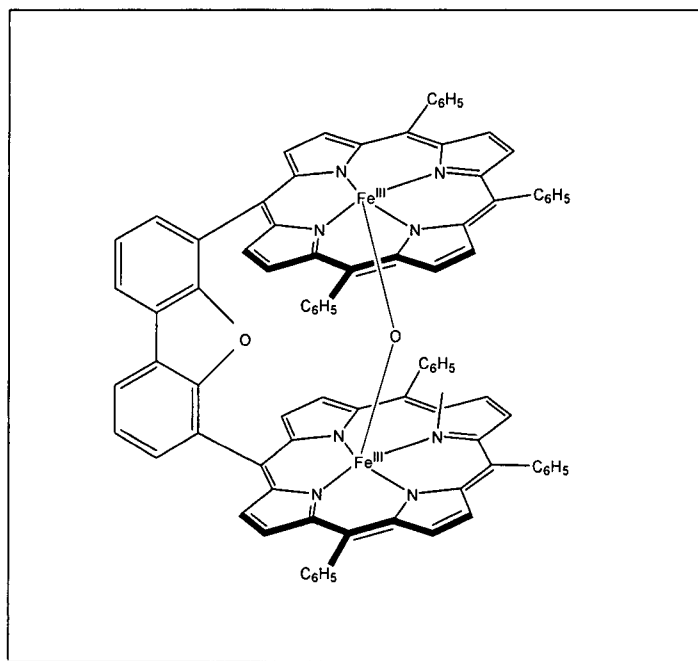
Scheme 6. "Pacman" diiron(III)-μ-oxo-bisporphyrin complex

This study has discovered that ruthenium(IV) μ-oxo bisporphyrin complexes catalyzed efficient aerobic oxidation of alkenes and activated hydrocarbons by the using visible light and atmospheric oxygen as oxygen source. The observed photocatalytic oxidation is ascribed to a photodisproportionation mechanism to afford a putative porphyrin-ruthenium(V)-oxo species that can be directly observed and kinetically studies by laser flash photolysis methods in further studies.[26,33]

II. GENERAL EXPERIMENTAL SECTION

2.1. <u>Materials & Chemicals</u>

All the organic solvents for synthesis and purification, including acetonitrile, methylene chloride, chloroform, hexane, ethyl acetate, methanol, acetone, ethanol and carbon tetrachloride, were of analytical grade and used as received without further purification. All reactive substrates for kinetic and photocatalytic studies were the best available purity from Aldrich Chemical Co., including 4-methoxy thioanisole, 4-methyl thioanisole, 4-fluorothioanisole, 4-chlorothioanisole, 4-bromothioanisole, thioanisole, styrene, *cis*-cyclooctene, diphenylmethane, cyclohexene, ethylbenzene, deuterium ethylbenzene-d_{10}, triphenylphosphine, benzophenone, xanthenes, xanthydrol, 1-phenylethanol, cumene, norbornylene, 1,2-dihydronaphthalene and cyclohexene. The pyrrole was obtained from Aldrich Chemical Co. and freshly distilled before use. 1,2,4-Trichlorobenzene was obtained from Sigma Aldrich and used as solvent and internal standard as well. Mesitaldehyde, boron trifluoride diethyl etherate (BF$_3$·OEt$_2$), 2,3-dichloro-5,6-dicyano-*p*-benzequinone (DDQ), *N*,*N*-dimethylformamide (DMF), 2,4,6-collidine, triethylamine, iodobenze diacetate, iodosobenzene (PhIO), 2,6-dichloropyridine, benzaldehyde, triruthenium dodecacarbonyl, decahydronaphthalene (decalin), *meta*-chloroperoxybenzoic acid (*m*-CPBA), 5,10,15,20-tetrakis(pentafluorophenyl)porphyrin [H$_2$(F$_{20}$-tpp)], 5,10,15,20-tetrakis(1-methyl-4-pyridinio)porphyrintetra(*p*-toluenesulfonate) (H$_2$TMPyP), anthracene, silver nitrate, silver perchlorate, silver chlorate, chloroform-*d*, acetonitrile-*d$_3$*, hydrogen peroxide, *tert*-butly

17

hydroperoxide (TBHP), deuterium hydrogen oxide, were purchased from Sigma-Aldrich and also used as received.

2.2. Physical Measurements

UV-vis spectra were recorded on an Agilent 8453 spectrophotometer, and kinetic studies were performed on the above spectrophotometer coupled with a Pro-K 2000 rapid stopped-flow mixing system (Applied Photophysics). Gas Chromatograph analyses were conducted on a Hewlett-Packard model HP 5890 Series II equipped with a flame ionization detector (FID) with DB-5 capillary column. The GC system is coupled with HP 7673 GC/SFC auto simple injector. Quantification of gas chromatographic fractions was conducted using a Agilent 3396 Series III integrator. Infra-red (IR) spectra were obtained using KBr on a Perkin Elmer Spectrometer. ^{1}H-NMR was performed on a JEOL ECA-500 MHZ spectrometer.

2.3. Reagents Purification

The pyrrole was purified by distillation according to the following procedure. Around 25 mL pyrrole measured by graduated cylinder was added into 50 mL round-bottomed flask which contained a magnetic spin vane. The solution was heated by a regulated heater. The distillation was conducted with a short-path apparatus from ChemGlass. Since boiling point of the pyrrole is around 129 °C, all the distillate collected below that temperature were abandoned. The freshly distilled colorless pyrrole was

directly used in synthesis of the free porphyrin ligand. The *N,N*-dimethylformamide (DMF) with 155 °C boiling was distilled following the similar procedure.

2.4. Kinetic Measurements

Kinetic measurements were performed on an Agilent 8453 diode array spectrophotometer interfaced with the Pro-K 2000 Rapid Mixing System by using standard 1.0-cm quartz cuvettes. The temperature of solution during kinetic experiments was retained to 23 ± 2 °C. The fast kinetic study of two-electron oxidations of *para*-substituted phenyl methyl sulfides was conducted spectroscopically by stopped-flow system which is a rapid mixing technique and able to detect the reactions in the time scale as short as 100 minisecond (ms.).

The rates of the reactions which represented the rates of oxo group transfer from $[Ru^{VI}(O)_2Por^*]$ to sulfides or alkenes were monitored by the decay of the Soret absorption band of the dioxoruthenium complex (λ_{max}). The pseudo-first order rate constants (k_{obs}) were obtained by nonlinear least-squares fits of (A_f -A_t) to time (t) according to the following equation:

$$(A_f - A_t) = (A_f - A_i)\exp(-k_{obs}t)$$

Where A_f and A_i are the final and initial absorbance, respectively, and A_t is the absorbance measured at time t. Based on the equation below, k_0 is a background rate constant found in the absence of substrate, [Sub] is the concentration of substrate, and the second-order

rate constants (k_2) were obtained as the slope from the linear fit of k_{obs} values to various concentrations of the substrates.

$$k_{obs} = k_0 + k_2[\text{Sub}]$$

2.5. Competitive Catalytic Oxidations

Various ruthenium porphyrins were investigated as the catalysts in the competitive oxidation reactions. A reaction solution containing equal amounts of two substrates, e.g., thioanisole (0.5 mmol) and substituted thioanisole (0.5 mmol), ruthenium(II) porphyrin catalyst (1 μmol) and an internal standard of 1,2,4-trichlorobenzene (0.5 mmol) was prepared (5 mL). The standard was shown to be stable to the oxidation conditions in control reactions. Iodosobenzene (PhIO) or *tert*-butly hydroperoxide (TBHP) (0.2 mmol) was added, and the mixture was stirred overnight (22h) under an inert atmosphere at $23 \pm 2\,^{\circ}\text{C}$. The amounts of substrates before and after the reactions were determined by GC analysis with DB-5 capillary column. Relative rate ratios for oxidations were determined based on the following equation.

$$k_{rel} = k_Y/k_H = \log(Y_f/Y_i)/\log(H_f/H_i)$$

where Y_f and Y_i are the final and initial quantities of the substituted thioanisole; H_f and H_i are the final and initial quantities of thioanisole.

2.6. Photocatalysis Procedure

trans-Dioxoruthenium(VI) porphyrin and bis-porphyrin-ruthenium(IV) μ-oxo dimer complexes were evaluated as the photocatalyst in the aerobic oxidation reactions. The reactions were typically carried out with 0.5 mg of catalyst in the 10 mL oxygen-saturated solution containing 2 ~ 4 mmol of substrates. In most cases, 5 ~ 10 mg of anthracene was added to enhance the catalytic activity. After 24 hours of photolysis with visible light (λ_{max} = 420 nm), a known amount of 1,2,4-trichlorobenzene was added as an internal standard for GC analysis. Oxidized products were analyzed by GC with DB-5 capillary column. Product identification is based on the commercially available authentic standards. Turnover number (TON) is calculated based on the following definition:

$$\text{TON} = \text{moles of products/ moles of catalyst}$$

III. SYNTHESIS, AND SPECTROSCOPIC CHARACTERIZATION OF RUTHENIUM PORPHYRIN COMPLEXES

3.1. Synthesis and Characterization of of *meso*-Tetramesitylporphyrin H₂TMP (1a)

The sterically encumbered free porphyrin ligand was prepared according to the well-known method described by Lindsey and co-workers,[34] as shown in Scheme 1. 1-L round-bottomed flask fitted with reflux condenser and nitrogen inlet port was charged with freshly distilled pyrrole (347 μL, 5 mmol, 10^{-2} M), mesitaldhyde (736 μL, 5 mmol, 10^{-2} M) and chloroform (500 mL). After the solution was purged with N_2 for 5 min, boron trifluoride diethyl etherate (BF₃·OEt₂) (660 μL, 1.65 mmol, 3.3×10^{-2} M) was added dropwise by syringe, and the solution was stirred for 1 h at room temperature. The reaction was monitored by removing 50 μL aliquot and oxidizing with excess 2,3-dichloro-5,6-dicyano-*p*-benzequinone (DDQ), followed by absorption spectrophotometry to confirm polypyrromethanes had been formed during the room temperature reaction. After the polypyrromethanes was formed, DDQ (957 mg) in power form was added and the reaction mixture was gently refluxed for 1 h. After the solution was cooled to room temperature, 1 equiv. of triethylamine (230 μL, 1.65 mmol) was added to neutralize the mixture, and the solution was evaporated to dryness. The solid crude product was placed on a filter and washed with a large excess of methanol under vacuum until the filtrate was clear. Since the polypyrromethanes and quinine components are highly soluble in the methanol and could be removed with ease. The further purification was performed by column chromatography (Silica gel). After placing the crude product into the wet column, dichloromethane was used to elute the product. The *meso*-tetramesitylporphyrin was obtained as purple solid after rotary evaporation. The designed porphyrin ligand H₂TMP

(**1a**) was characterized by UV-vis (Figure 3) and ^{1}H-NMR (Figure 4), consistent with those literature reported.[34]

[H$_2$TMP] (**1a**). Yield = 25.6%. ^{1}H-NMR (300MHz, CDCl$_3$): δ, ppm: -2.51 (br s, 2H, NH), 1.81 (s, 24H, o-CH$_3$), 2.62 (s, 12H, p-CH$_3$), 7.26 (s, 8H, m-ArH), 8.61 (s, 8H, β-pyrrole). UV-vis (CH$_2$Cl$_2$) λ_{max}/nm: 418 (Soret), 441, 513, 546, 594, 645.
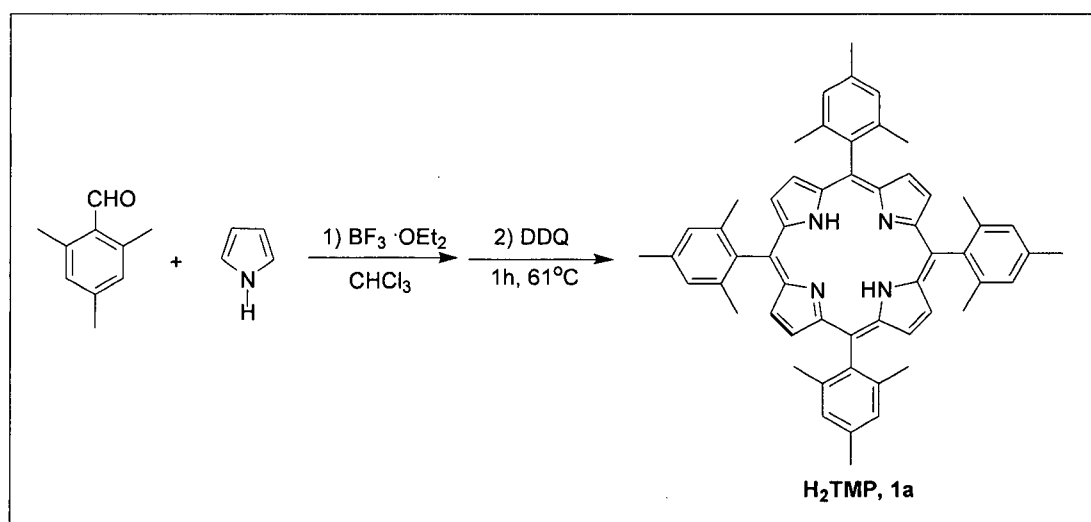
Scheme 7. Synthesis of H$_2$TMP (**1a**).
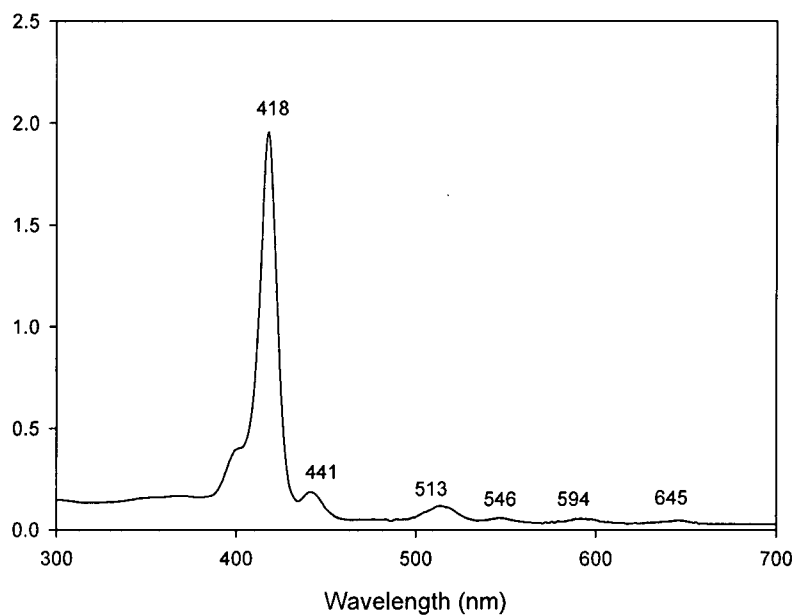
Figure 3. The UV-vis spectrum of H_2TMP (**1a**) in CH_2Cl_2.
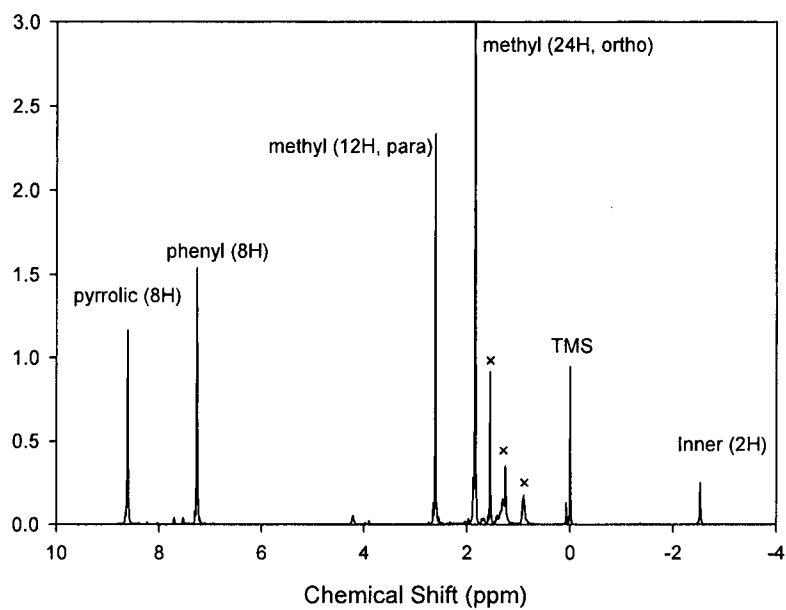
Figure 4. The ^{1}H-NMR spectrum of H_2TMP (**1a**) in $CDCl_3$.

3.2. Synthesis and Characterization of Carbonyl Ruthenium(II) Porphyrin Complexes (2)

According to the literature method described by Che and co-workers,[35] carbonyl ruthenium (II) porphyrin complexes were synthesized by the following procedure.[33] H_2TMP (**1a**) (150 mg) was placed in a 100 mL round-bottom flask with decalin (50 mL) as solvent when the reaction is gently heated with stirring to ca. 100 °C. Excess triruthenium dodecacarbonyl [$Ru_3(CO)_{12}$] (150 mg) was added and the solution was refluxed at 180 °C for 1 hour. UV-vis spectroscopy was used to confirm the Soret band of the metal complex product according to the literature values. The mixture was cooled to room temperature and an alumina oxide basic column was used for product separation and purification. The column was loaded by crude product followed by excess hexane to remove the high-boiling-point decalin. Dichloromethane was then utilized to elute the unreacted free ligand and product, respectively. The brick-red solid was obtained after the solvent was removed via rotary evaporation. The desired metalloporphyrin $Ru^{II}(CO)TMP$ (**2a**) was fully characterized by UV-vis (Figure 5), IR (Figure 6) and ^1H-NMR (Figure 7), matching those literature reported.[36]

[$Ru^{II}(CO)TMP$] (**2a**). Yield = 61.5%. ^1H-NMR (300 MHz, $CDCl_3$): δ, ppm: 1.84 (s, 24H, o-CH_3), 2.60 (s, 12H, p-CH_3), 7.24 (s, 8H, m-ArH), 8.45 (s, 8H, β-pyrrole).

IR (KBr, cm^{-1}): 1934 (v_{Ru-CO}), 1010 cm^{-1} (oxidation state marker band). UV-vis (CH_2Cl_2) λ_{max}/nm: 412 (Soret), 530.
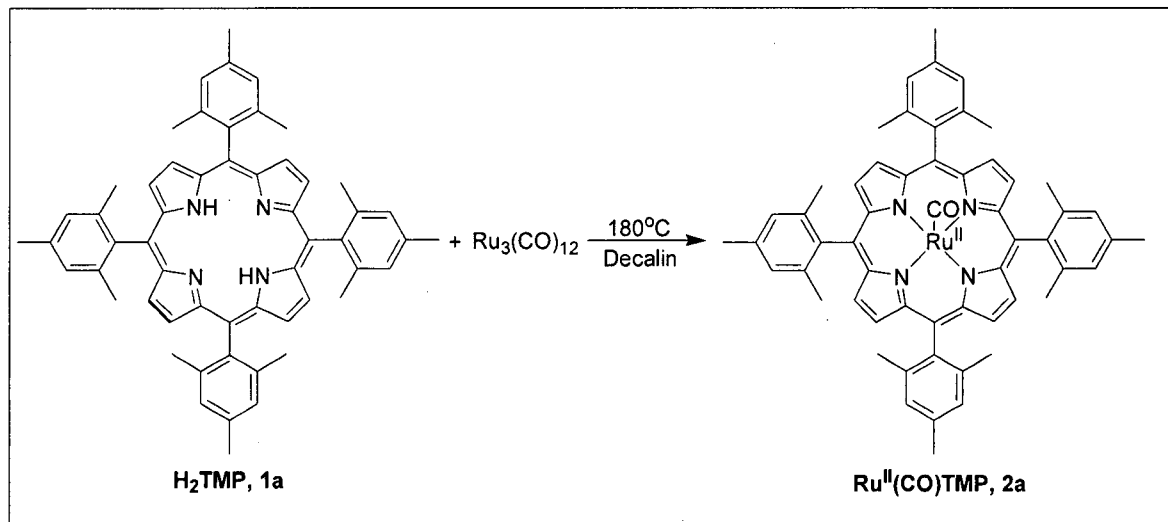
Scheme 8. Synthesis of Ru^{II}(CO)TMP (**2a**).
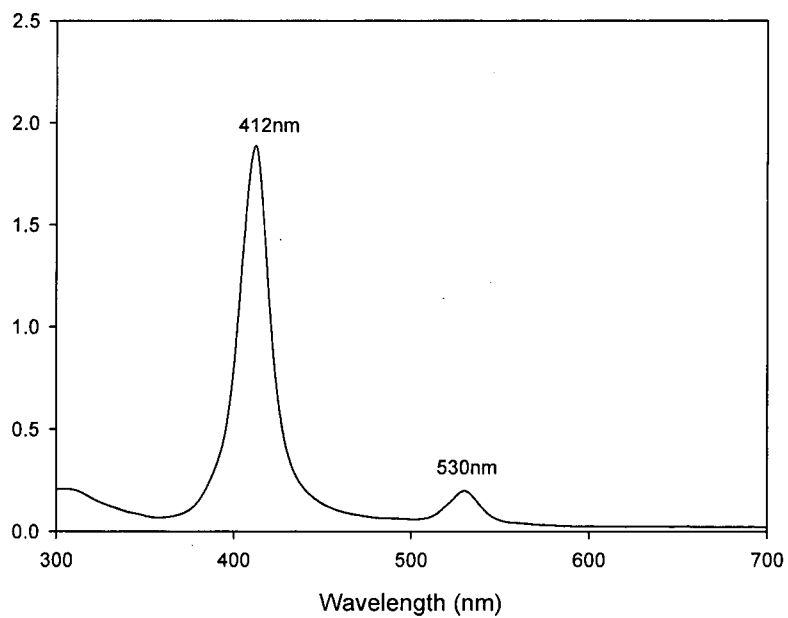
Figure 5. The UV-vis spectrum of Ru^{II}(CO)TMP (**2a**) in CH$_2$Cl$_2$.
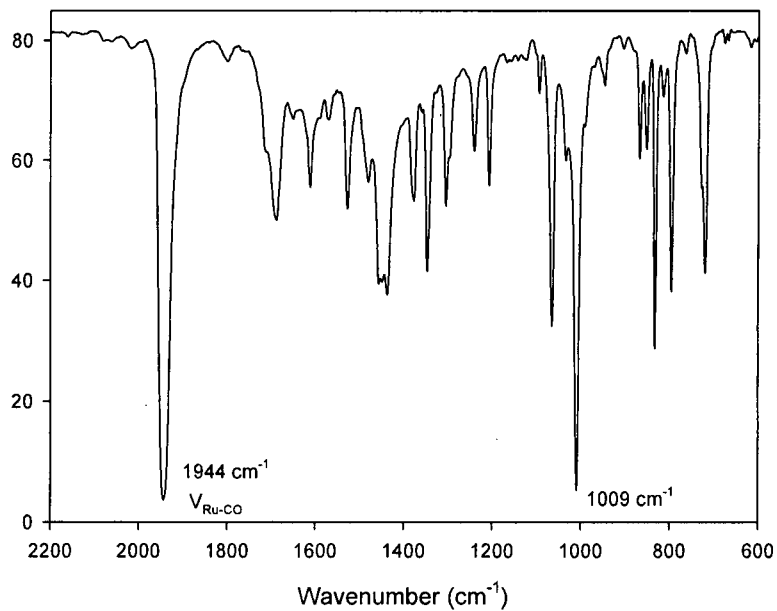
Figure 6. The IR spectrum of $Ru^{II}(CO)TMP$ (**2a**) (KBr).
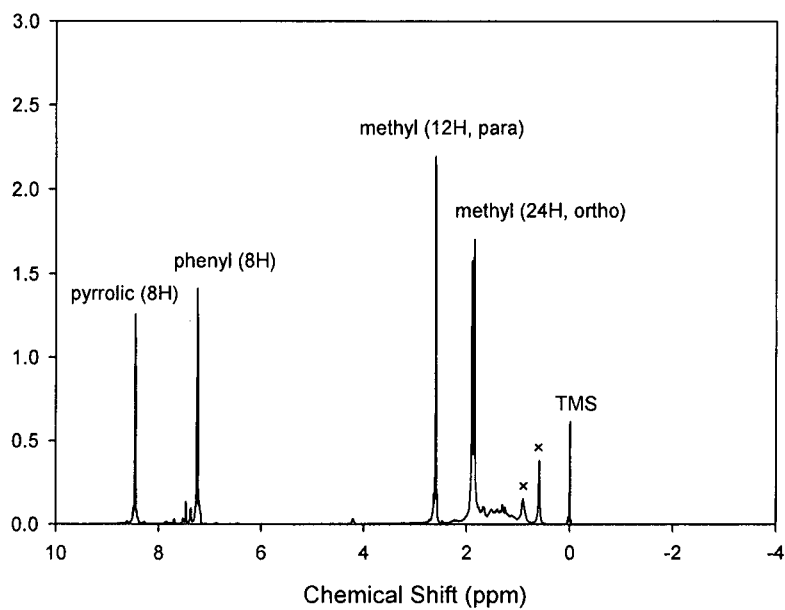
Figure 7. The ^{1}H-NMR spectrum of $Ru^{II}(CO)TMP$ (**2a**) in $CDCl_3$.

In a fashion similar to that described for the generation of Ru^{II}(CO)TMP, the
electron-deficient Ru^{II}(CO)TPFPP (**2b**) was also prepared. Since the electron-deficient
Ru^{II}(CO)TPFPP contains more electron-withdrawing groups that required higher reaction
temperature, 1,2,4-trichlorobenzene was used instead of decalin for the synthesis of **2b**.
The use of the more polar 1,2,4-trichlorobenzene at a higher temperature (220°C) in the
synthesis of **2b** resulted in a better yield compared to the non-polar solvent decalin. The
desired product Ru^{II}(CO)TPFPP (**2b**) was fully characterized by UV-vis (Figure 8), IR
(Figure 9) and ^{1}H-NMR (Figure 10), matching those literature reported.[36]

[Ru^{II}(CO)TPFPP] (**2b**). Yield = 93%. ^{1}H-NMR (300 MHz, CDCl$_3$): δ, ppm: 8.71 (s, 8H,
β-pyrrole). IR (KBr): 1963 cm^{-1} (v_{Ru-CO}), 1009 cm^{-1} (oxidation state marker band). UV-
vis (CH$_2$Cl$_2$) λ_{max}/nm: 402 (Soret), 524.
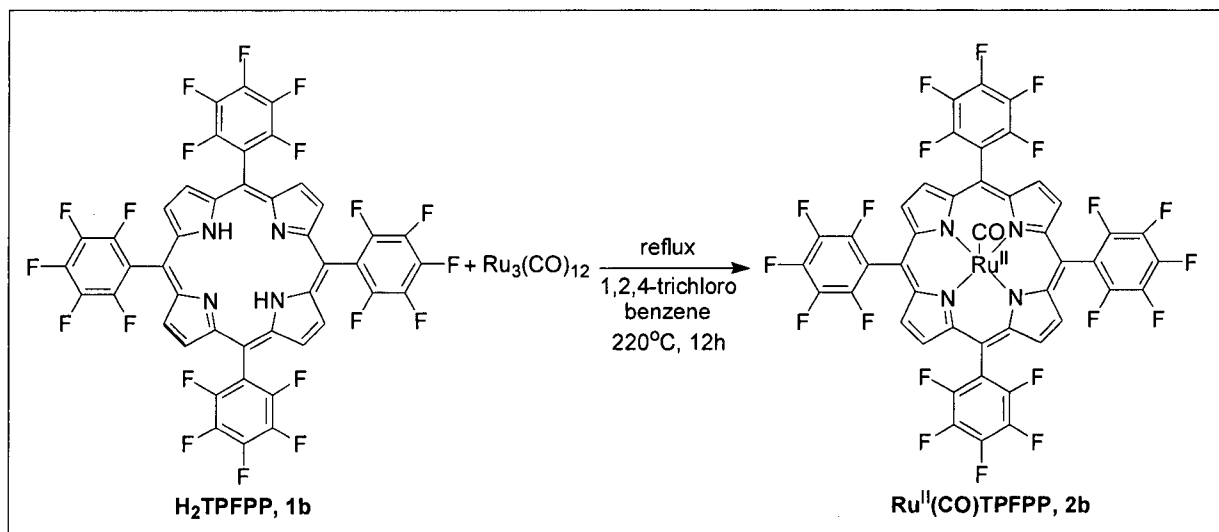
Scheme 9. Synthesis of Ru^{II}(CO)TPFPP (**2b**).
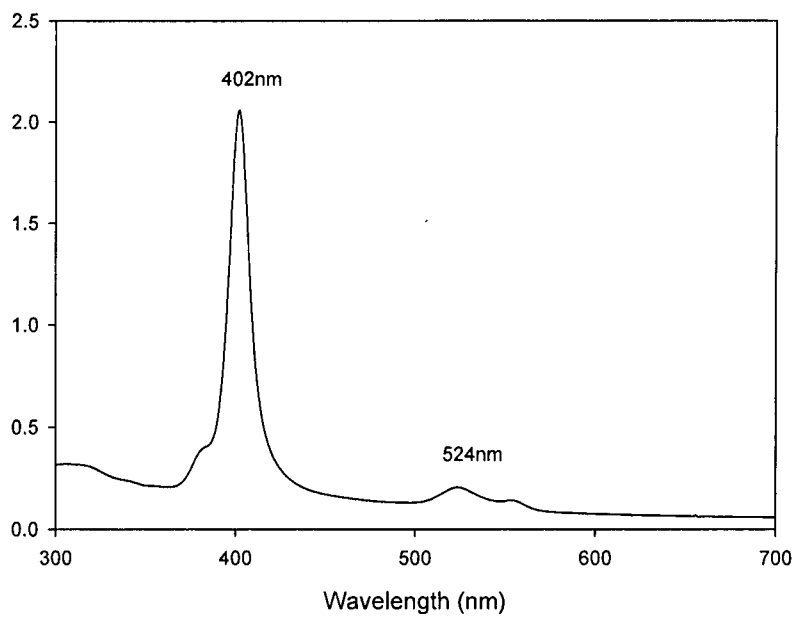
Figure 8. The UV-vis spectrum of Ru^{II}(CO)TPFPP (**2b**) in CH$_2$Cl$_2$.
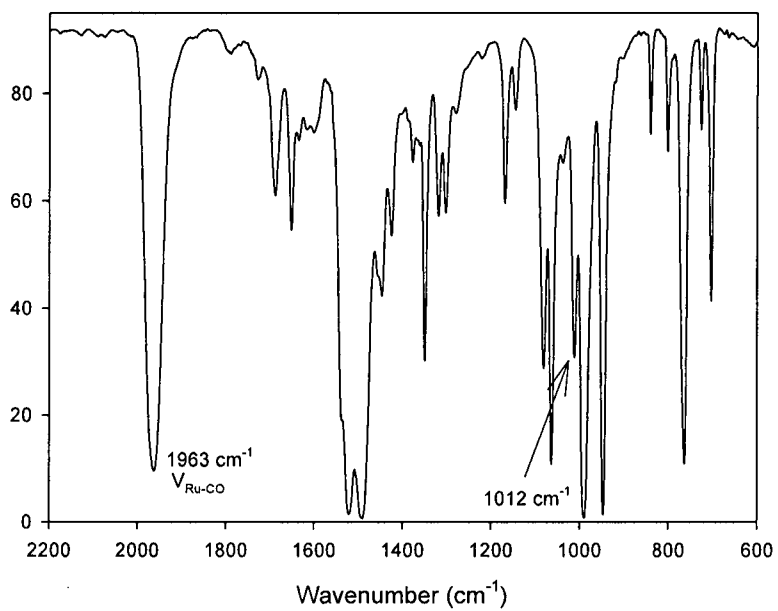
Figure 9. The IR spectrum of Ru^{II}(CO)TPFPP (**2b**) (KBr).
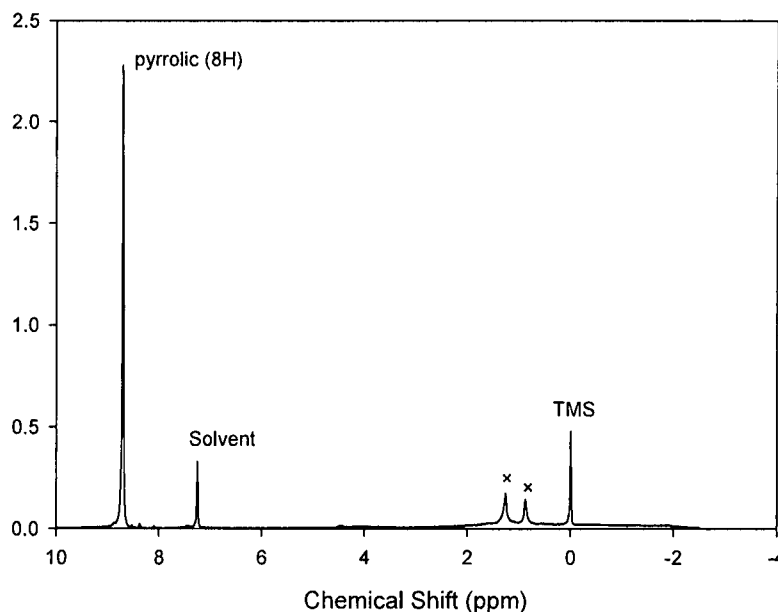
Figure 10. The ^{1}H-NMR spectrum of Ru^{II}(CO)TPFPP (**2b**) in CDCl$_3$.

Following the literature method reported by Hartmann and co-workers, water

soluble ruthenium complex was also prepared.[37] A suspension of H$_2$TMPyP (100 mg)

that was dissolved in freshly distilled DMF (40 mL) and 2,4,6-collidine (0.25 mL, 1.9

mmol, 12 equiv.) was heated to reflux at 155 °C with magnetic stirring vane.

Triruthenium dodecacarbonyl [Ru$_3$(CO)$_{12}$] (100 mg, 1 equiv.) was added when the

solvent was almost refluxed. UV-visible spectroscopy was used to monitor the process by

checking aliquot of diluted reaction solution in dichloromethane/ trifluoroacetic acid

(95/5, v/v) whether the disappearance of the Soret band due to [H$_2$TMPyP] (423 nm) and

the increase of the soret band at 420 nm and Q band (536 nm). After cooling of the

reaction mixture, the crude product was washed by excess hexane to remove the

remaining 2,4,6-collidine and organic impurity, and then washed by dichloromethane

twice until filtrate was colorless. By using CH_3CN which could dissolve the crude

product, impurities such as Ru^{3+} and Cl^- were removed. The brick-red solid was obtained

after the acetonitrile was removed by rotary evaporation. The desired complex

$Ru^{II}(CO)TMPyP$ (**2c**) was characterized by UV-vis (Figure 11), IR (Figure 12) and ^1H-

NMR (Figure 13).

$[Ru^{II}(CO) TMPyP]$ (**2c**). Yield = 79.3%. ^1H-NMR (300MHz, CD_3CN): δ, ppm: 9.08 (m,

8H, β-pyrrole), 8.76 (s, 8H), 4.64 (s, 12H, N^+-CH_3). UV-vis (CH_3CN) λ_{max}/nm: 422

(Soret), 538.
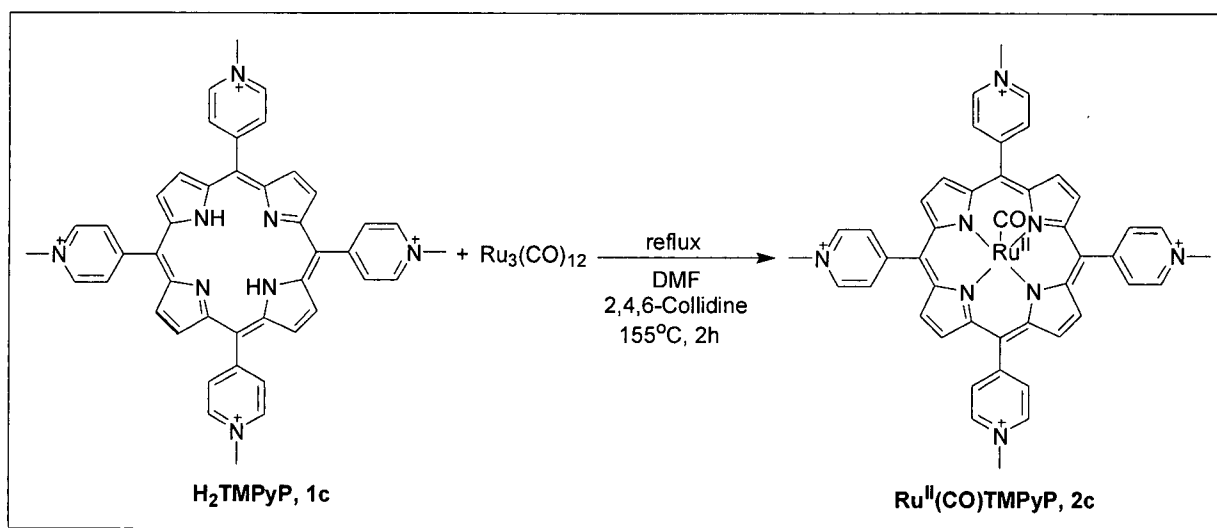
Scheme 10. Synthesis of $Ru^{II}(CO)$ TMPyP (**2c**).
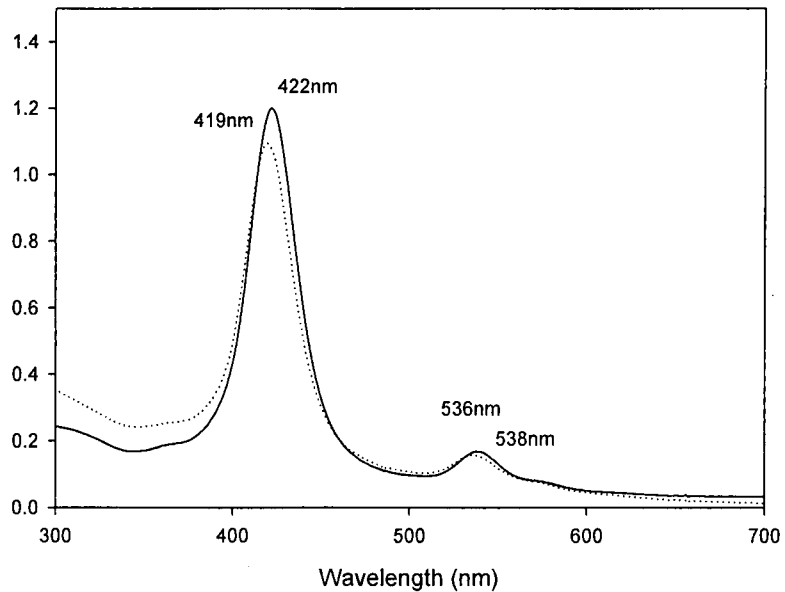
Figure 11. The UV-vis spectrum of Ru^{II}(CO)TMPyP (**2c**) (solid line) in CH$_3$CN and **2c** (dotted line) in H$_2$O.
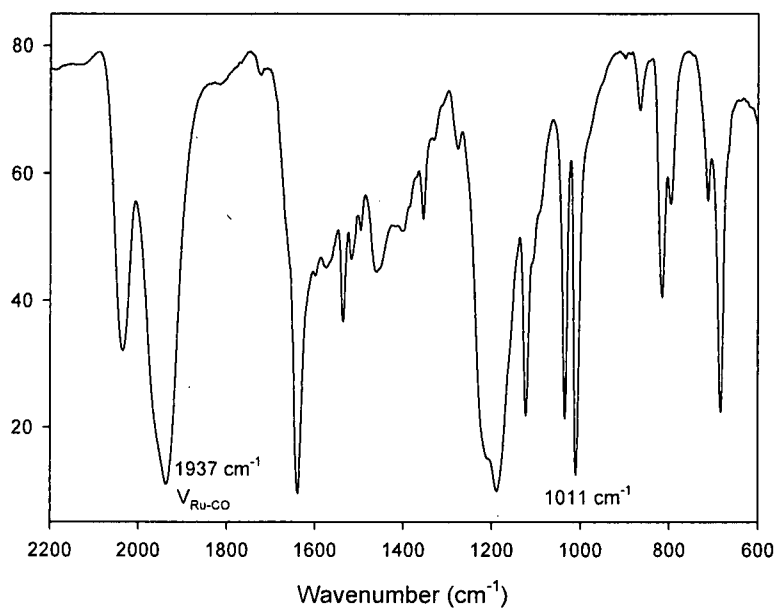
Figure 12. The IR spectrum of Ru^{II}(CO)TMPyP (**2c**) (KBr).
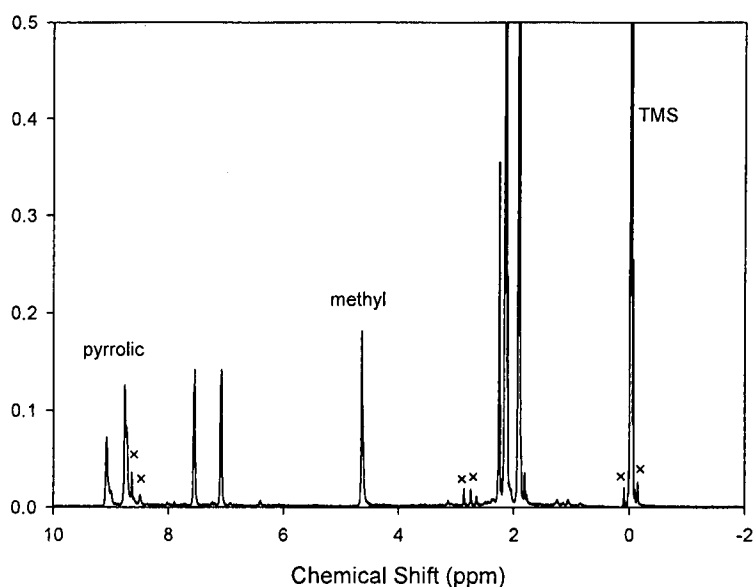
Figure 13. The ^{1}H-NMR spectrum of Ru^{II}(CO)TMPyP (**2c**) in CD$_3$CN.

3.3 Synthesis and Characterization of *trans*-Dioxoruthenium(VI) Porphyrin Complexes(3)

A dichloromethane solution of [Ru^{II}(Por)(CO)(MeOH)] (2 mg) was added to a well-stirred solution of *meta*-chloroperoxybenzoic acid (*m*-CPBA) (3 mg) in CH$_2$Cl$_2$ (1 mL) at room temperature.[38] After stirring for 3-5 min, the resultant solution was loaded on a short alumina column for purification. Chloroform or dichloromethane was used to elute the desired product. The dark-purple solid product, *trans*-dioxo-(5,10,15,20-tetrakismesitylporphyrinato ruthenium(VI) (Ru^{VI}(O)$_2$TMP, **3a**), was obtained after the solvent was removed by rotary evaporation. The Ru^{VI}(O)$_2$TMP (**3a**) was fully characterized by UV-vis (Figure 14), IR (Figure 15) and ^{1}H-NMR (Figure 16), matching those reported.[38]

[Ru^{VI}(O)$_2$TMP] (**3a**). Yield = 92%. ^{1}H-NMR (300 MHz, CDCl$_3$) δ, ppm: 1.89 (s, 24H, *o*-CH$_3$), 2.62 (s, 12H, *p*-CH$_3$), 7.23 (s, 8H, *m*-ArH), 8.79 (s, 8H, *β*-pyrrole).

IR (KBr, cm^{-1}): 1018 (oxidation state marker band) and 819 (ν$_{O=Ru=O}$). UV-vis (CH$_2$Cl$_2$) λ$_{max}$/nm: 422 (Soret), 521.
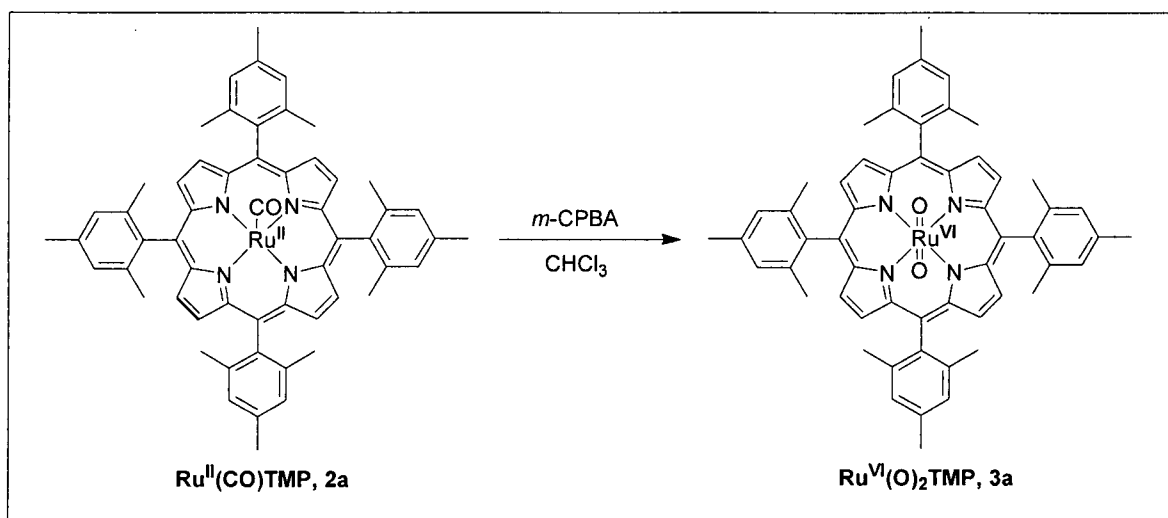
Scheme 11. Synthesis of Ru^{VI}(O)$_2$TMP (**3a**).
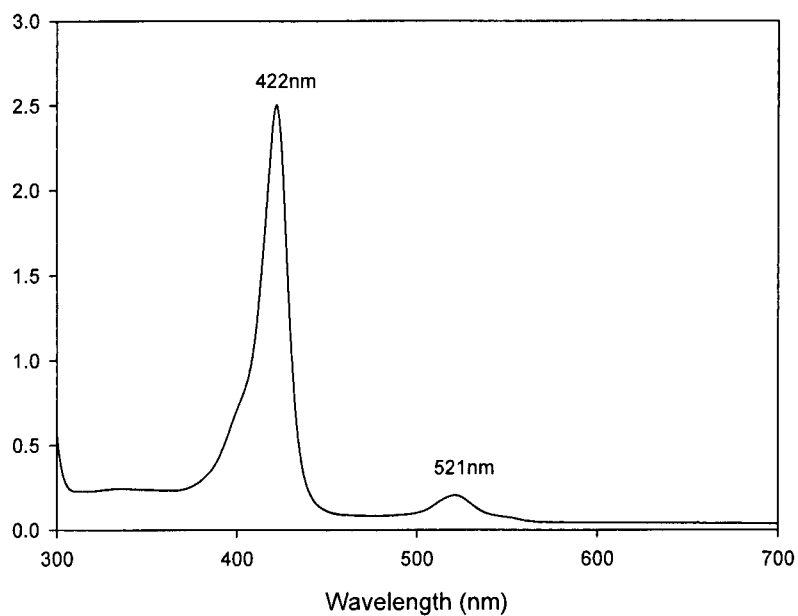
Figure 14. The UV-vis spectrum of $Ru^{VI}(O)_2TMP$ (**3a**) in CH_2Cl_2.
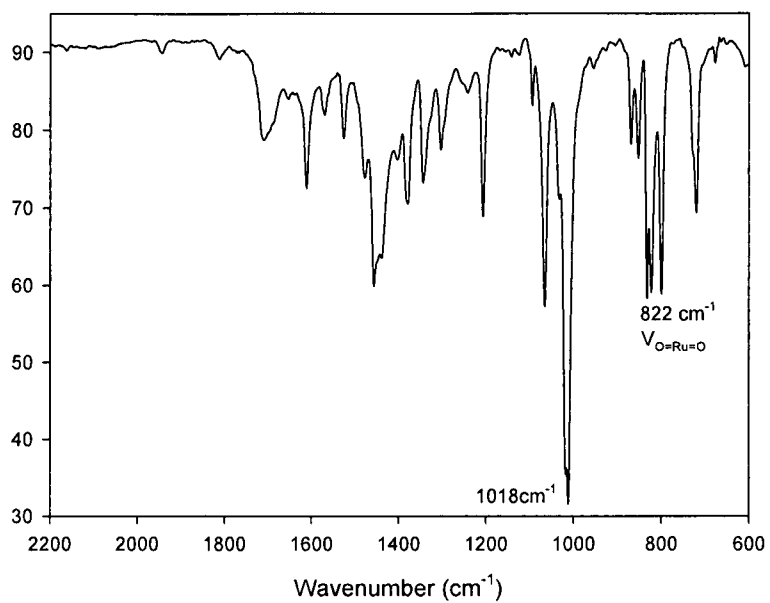
Figure 15. The IR spectrum of $Ru^{VI}(O)_2TMP$ (**3a**) (KBr).
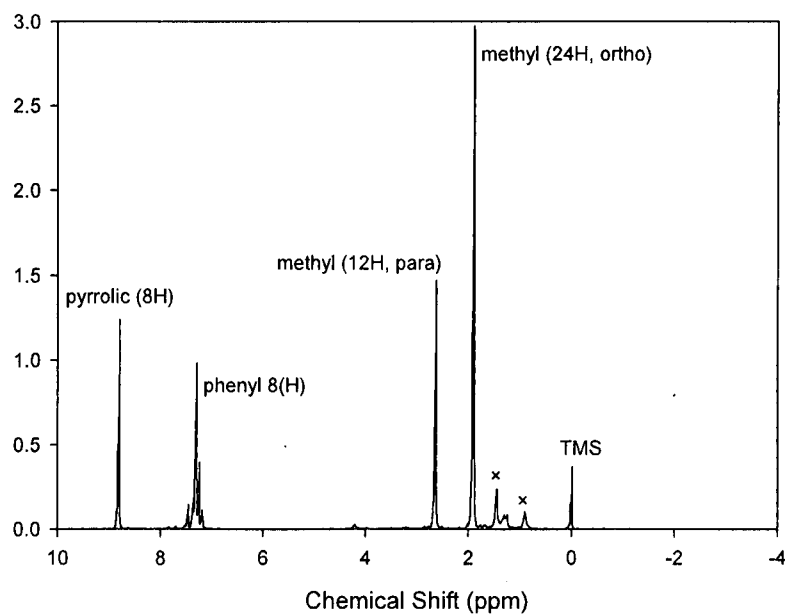
Figure 16. The ^{1}H-NMR spectrum of $Ru^{VI}(O)_2TMP$ (**3a**) in $CDCl_3$.

In a fashion similar to that described for the generation of $Ru^{VI}(O)_2TMP$, the electron-deficient $Ru^{VI}(O)_2TPFPP$ (**3b**) was also prepared and characterized.

$[Ru^{VI}(O)_2TPFPP]$ (**3b**). Yield = 90%. ^{1}H-NMR (300 MHz, $CDCl_3$): δ, ppm: 9.18 (s, 8H, β-pyrrole). IR (KBr, cm^{-1}): 1022 (oxidation state marker band) and 827 ($v_{O=Ru=O}$). UV-vis (CH_2Cl_2) λ_{max}/nm: 413 (Soret), 506.
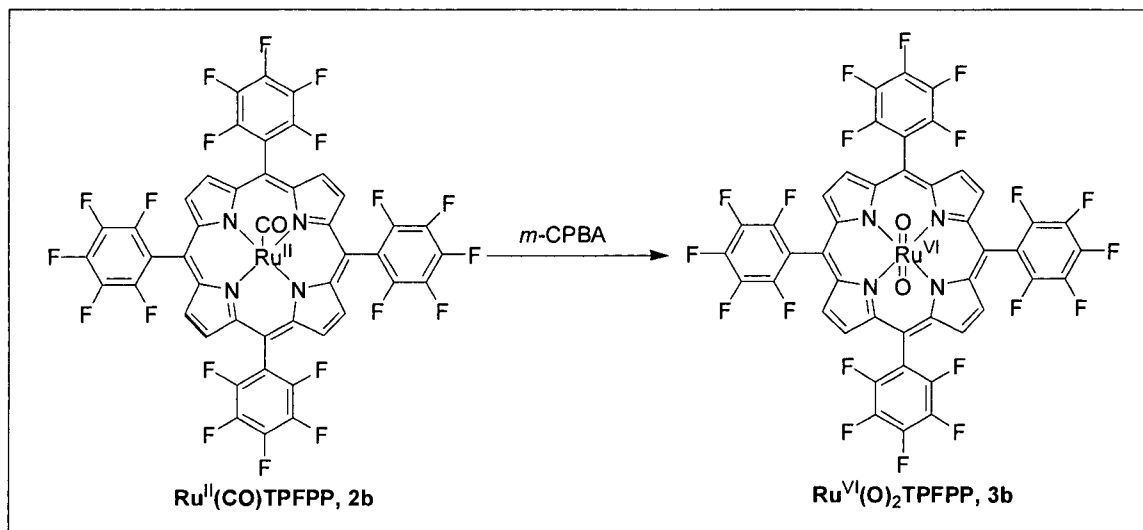
Scheme 12. Synthesis of $Ru^{VI}(O)_2TPFPP$ (**3b**).
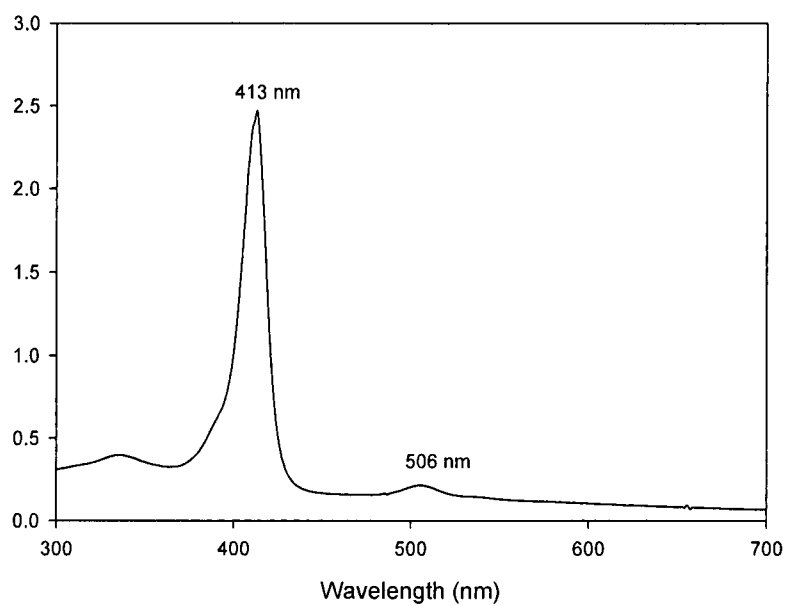
Figure 17. The UV-vis spectrum of $Ru^{VI}(O)_2TPFPP$ (**3b**) in CH_2Cl_2.
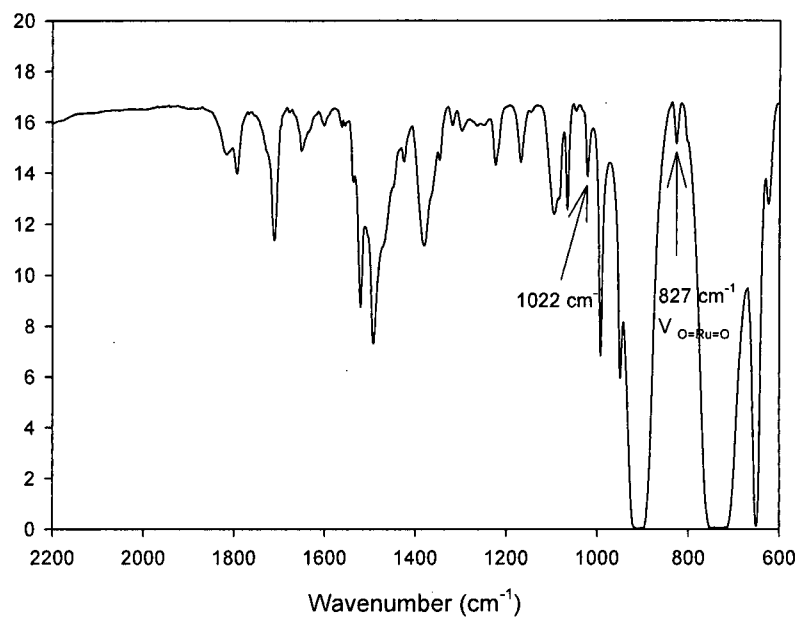
Figure 18. The IR spectrum of $Ru^{VI}(O)_2TPFPP$ (**3b**) (KBr).
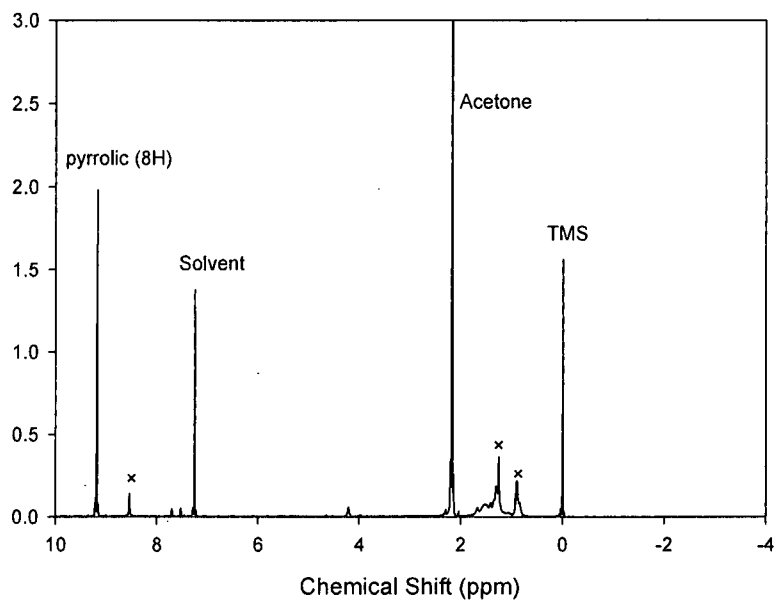
Figure 19. The ^1H-NMR spectrum of $Ru^{VI}(O)_2TPFPP$ (**3b**) in $CDCl_3$.

3.4. Development of a Novel Photosynthesis of *trans*-Dioxoruthenium(VI) Porphyrins

In this work, a new photochemical method that led to generation of the dioxoruthenium(VI) porphyrin complexes bearing sterically hindered porphyrin ligand was also successfully developed.[20] The new photo protocol is shown in Scheme 13.
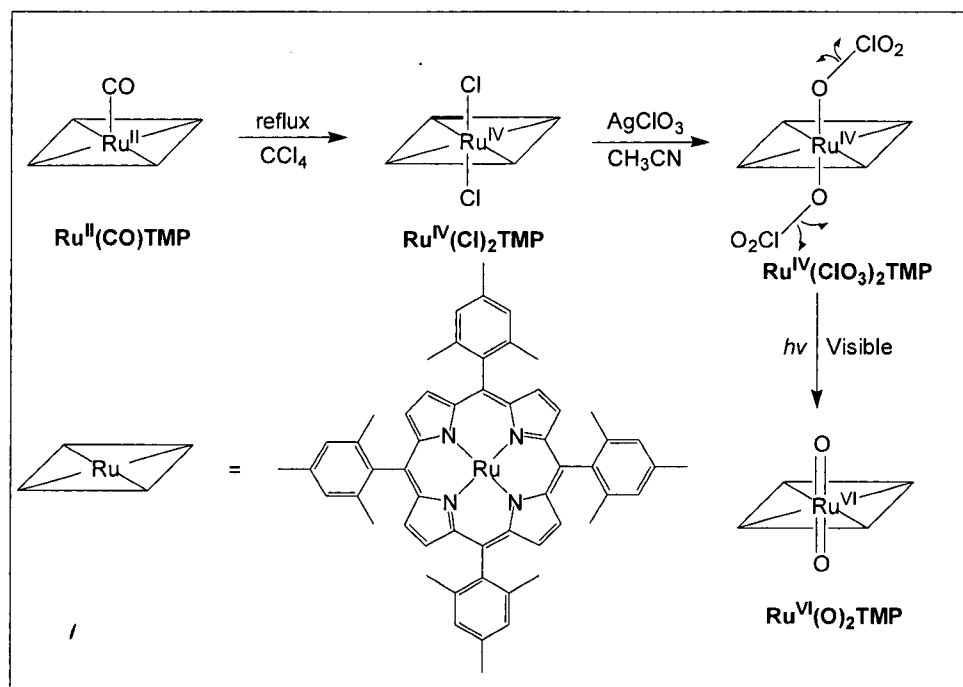
Scheme 13. Photosynthesis of $Ru^{VI}(O)_2TMP$ (**3a**).

According to the method developed by Gross and co-workers[39], the $Ru^{IV}(Cl)_2TMP$ (**4a**) was first prepared by heating $Ru^{II}(CO)TMP$ (**2a**) in refluxing CCl_4. The solid product directly obtained by removing the solvent. The complex **4a** was known and characterized by distinct paramagnetic ^1H-NMR (see Figure 22, paramagnetically shifted pyrrolic protons at δ -55.8 ppm in $CDCl_3$) in agreement with that reported.[39] The complex was also characterized by UV-visible spectra (Figure 20) and IR (Figure 21).
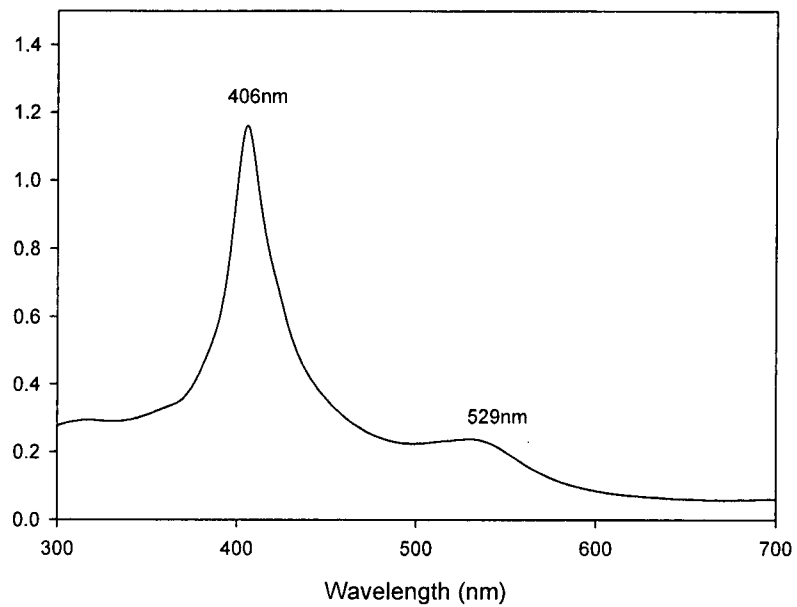
Figure 20. The UV-vis spectrum of $Ru^{IV}(Cl)_2TMP$ (**4a**) in CH_2Cl_2.
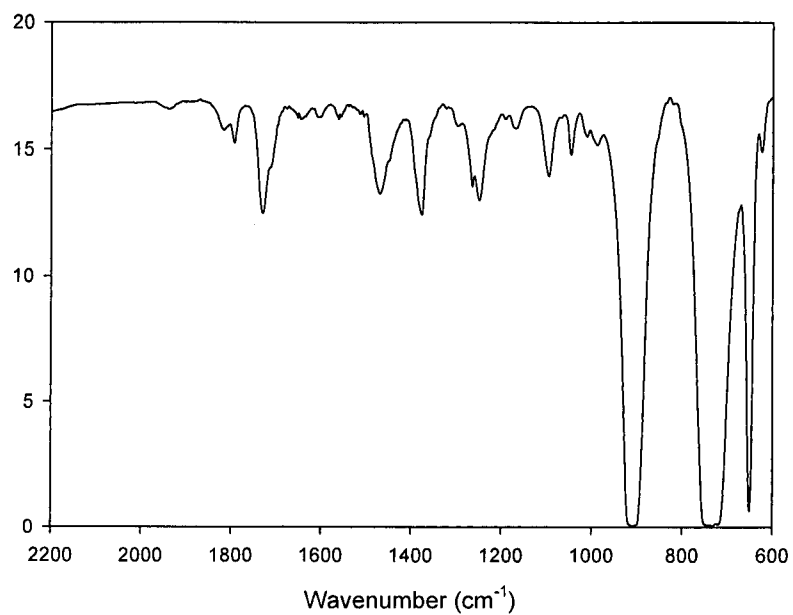
Figure 21. The IR spectrum of $Ru^{IV}(Cl)_2TMP$ (**4a**) (KBr).
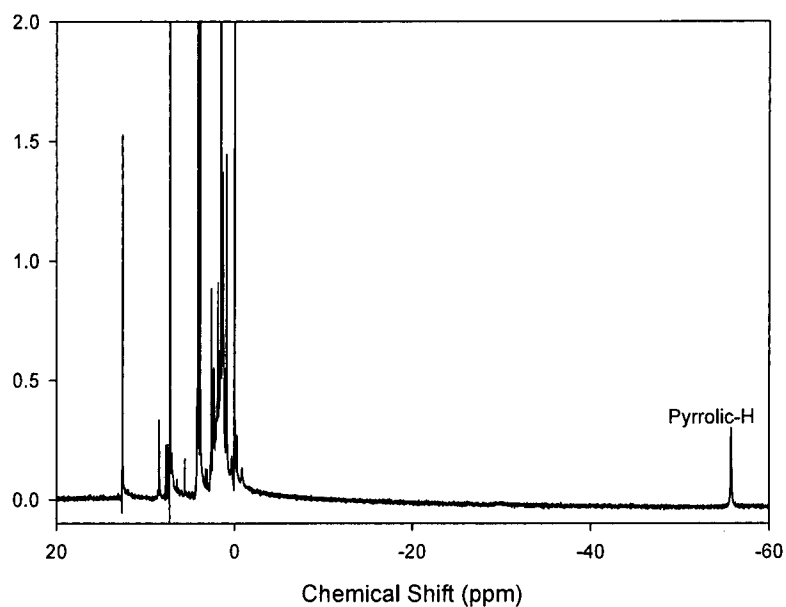
Figure 22. The ^{1}H-NMR spectrum of Ru^{IV}(Cl)$_2$TMP (**4a**) in CDCl$_3$.

Exchange of the counterions in Ru^{IV}(Cl)$_2$TMP with AgClO$_3$ gave the corresponding dichlorate salts Ru^{IV}(ClO$_3$)$_2$TMP (**5a**) that was desired photo labile precursor and subsequently used for photochemical reactions. The paramagnetic ^{1}H-NMR and UV-vis spectrum of intermediate **5a** was shown in Figure 23 and 24.
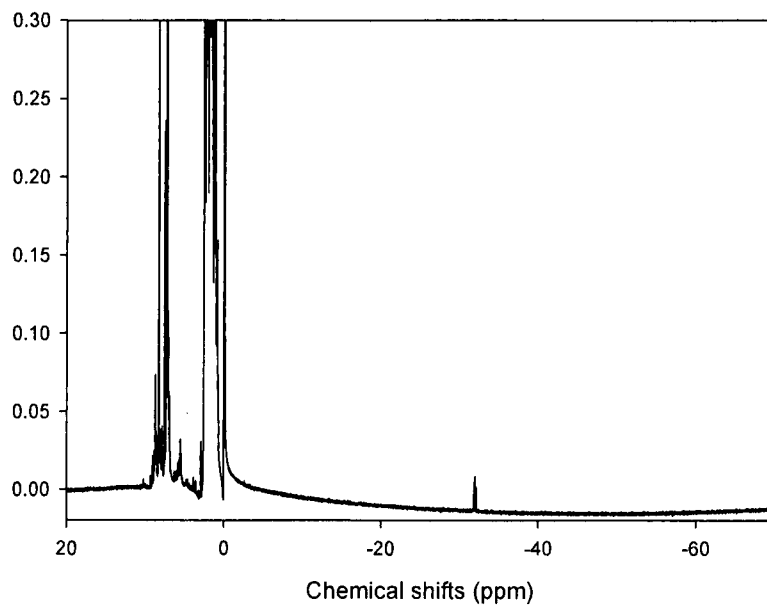
Figure 23. ^{1}H-NMR spectrum of $Ru^{IV}(ClO_3)_2TMP$ (**5a**) in $CDCl_3$.
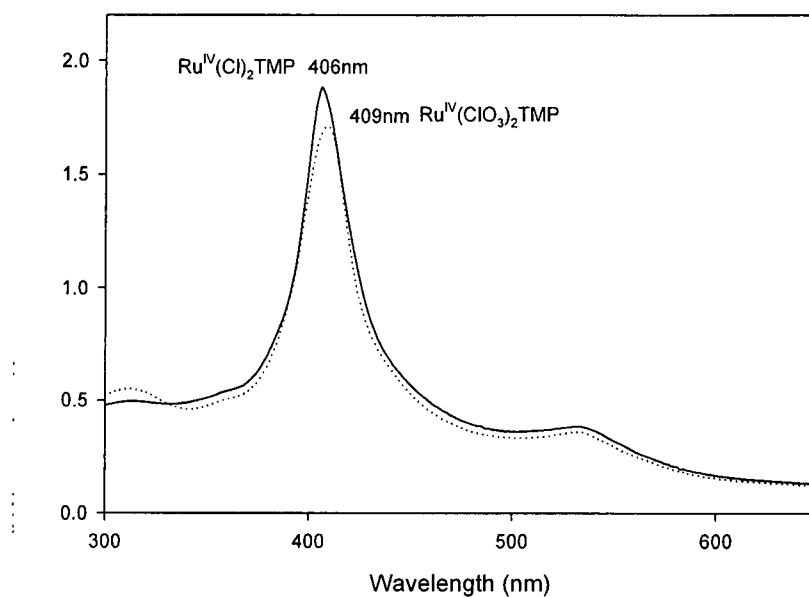
Figure 24. UV-visible spectra of $Ru^{IV}(Cl)_2TMP$ (**4a**, solid) and $Ru^{IV}(ClO_3)_2TMP$ (**5a**, dotted) in CH_3CN.

Irradiation of **5a** in anaerobic CH_3CN with visible light from a tungsten lamp resulted in changes in absorption spectra with isosbestic points at 338 nm, 412 nm, 436 nm, 593 nm (Figure 25). In Figure 25, **5a** was decayed and a new species was produced displaying a stronger soret band at 420nm and weaker Q band at 520nm that is characteristic for $Ru^{VI}(O)_2TMP$ (**3a**). The spectra signature of **3a** was further confirmed by ^1H-NMR and IR. Control experiments showed that no dioxo species was formed in the absence of light. Therefore, the photolysis reactions of **5a** undergo the homolytic cleavage of the O-Cl bond in the two chlorate counterions simultaneously to produce **3a** via two one-electron photooxidation pathways.[20]
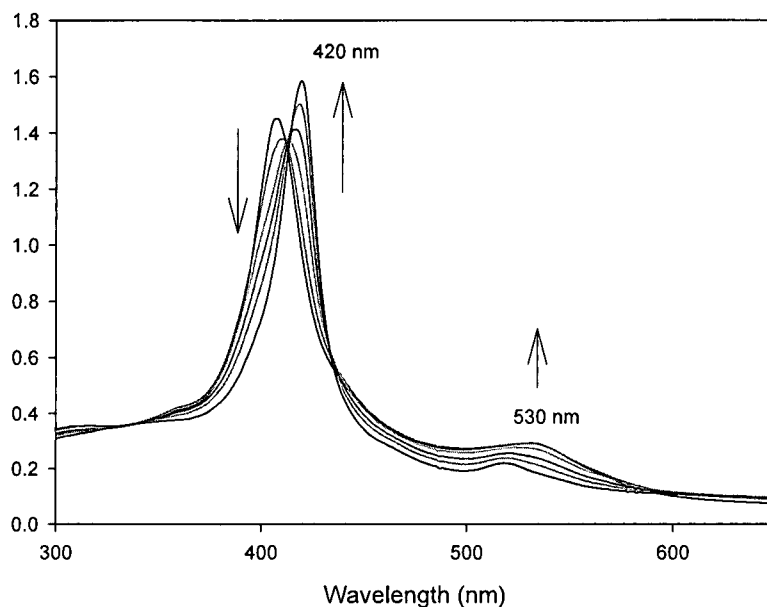
Figure 25. UV-visible spectral change of $Ru^{IV}(ClO_3)_2TMP$ upon irradiation with a 100W tungsten lamp in anaerobic CH_3CN solution at 22°C. Spectra were recorded at t = 0, 6, 14, 20, 26 and 50 min.

3.5. <u>Discussion</u>

3.5.1. <u>Synthesis</u>

The synthesis of the free ligands and the various ruthenium porphyrin complexes are well documented in the literature.[34,35,37-39] As reported by Lindsey et al., the yield and rate of the condensation of pyrrole and mesitaldehyde to form H_2TMP (**1a**) depends on a number of factors such as the solvent, the temperature, catalyst, cocatalyst, and the concentrations of reactants and catalysts.[34] As a result, although, a 25.6 % yield of **1a** might not represent the highest yield, the reported procedure presented the most convenient method for rapidly and producible obtaining a sterically encumbered porphyrin ligand with > 95% purity.

Insertion of ruthenium metal into porphyrins usually occurs readily upon treating $Ru_3(CO)_{12}$ with free-base porphyrins in an inert solvent to yield the corresponding ruthenium(II) carbonyl complexes. The choice of the solvent played an important role in the process of synthesis of ruthenium(II) carbonyl complexes. Following the procedures reported by Che and coworkers,[35] decalin was used as solvent in the synthesis $Ru^{II}(CO)TMP$ (**2a**). However, with the same solvent the reaction of H_2TPFPP with $Ru_3(CO)_{12}$ gave very low yield of $Ru^{II}(CO)TPFPP$ (**2b**). Finally, 1,2,4-trichlorobenzene was found to be the solvent of the choice, and **2b** was obtained in high yield. This solvent is found to be very useful for the preparation of polyfluorinated ruthenium porphyrin complexes since those kinds of complexes required more polar and higher boiling point solvent in the process of metal insertion.[36] According to the procedures described by Meunier et al.,[37] the water-soluble ruthenium porphyrins $Ru^{II}(CO)TMPyP$ was

synthesized by using freshly distilled *N,N*-dimethylformamide (DMF) as solvent because of its miscibility with water and the majority of organic liquids.

Recently, *trans*-dioxoruthenium(VI) porphyrins complexes have been received much attention, and developed as the well-characterized model system for heme-containing enzymes. The first isolation and characterization of the *trans*-dioxoruthenium(VI) porphyrins was reported by Groves and Quinn.[38] The sterically hindered carbonyl ruthenium complex (**2a-b**) was oxidized by *m*-CPBA yielded the corresponding *trans*-dioxoruthenium complex (**3a-b**). These dioxoruthenium(VI) complexes are stable enough for chromatographic purification on an alumina column using CH_2Cl_2 as the eluant and the spectroscopically pure complexes (**3a-b**) are obtained in *ca.* 70~90% yield. They are also low-reactivity intermediates that are suitable for the kinetic studies.[40] These relatively stable metal-oxo intermediates can be stored at -20°C for days.

Unlike the commonly used chemical oxidations, a novel photosynthesis of *trans*-dioxoruthenium(VI) porphyrins was developed in this work.[20] The new method used the photo-induced ligand cleavage reactions for production of the well-established *trans*-dioxoruthenium(VI) derivatives. The photochemical approach produced metal-oxo species essentially instantly, and permitted direct detection of ruthenium-oxo species and kinetic studies of their oxidations within much shorter timescales than the fastest mixing experiments.[41] In this study, the progress in the development of a new and extremely easy photochemical method that leads to generation of the dioxoruthenium(VI) complexes. The generality of the methodology was also demonstrated in sterically encumbered and unencumbered systems under same conditions, bypassing the ligand limitation observed

in chemical methods.[20] Furthermore, these promising results are expected to stimulate the further exploration of photo-synthetic methodology to produce other high-valent metal-oxo complexes.

3.5.2. UV-visible Spectra of the Ruthenium Porphyrins

The UV-visible spectral data of the ruthenium porphyrins are summarized in Table 1, and typical spectra are shown in Figures 3 (**1a**), 5 (**2a**), 8 (**2b**), 11 (**2c**), 14 (**3a**), 17 (**3b**), 20 (**4a**) and 24 (**5a**). In general, the UV-visible spectra of $[Ru^{II}(CO)Por^*)]$ and $[Ru^{VI}(O)_2(Por^*)]$ are typically featured by the Soret band due to $\pi - \pi^*$ electron transfer and a less intense Q band because of $n - \pi^*$ interaction. The spectrum of **1a** shows a strong signal for the Soret band and several less intense signals for the Q band which is typical of a normal free-base porphyrin ligand. Comparing with the positions of absorbance band of $[Ru^{II}(CO)Por^*)]$ and the corresponding $[Ru^{VI}(O)_2(Por^*)]$, the Soret bands are red-shifted by about 10 nm, however, the Q bands are blue-shifted.

Table 1. UV-vis Spectral Data of Ruthenium Porphyrin Complexes in $CH_2Cl_2/CHCl_3$ at Room Temperature

Compound	λ_{max} /nm	
	Soret bands	Q bands
1a	418	441, 513, 546, 594, 645
2a	412	530
2b	402	524
2c	422	538
3a	422	521
3b	413	506
4a	406	529
5a	409	531

3.5.3. Infrared Spectroscopy of the Ruthenium Porphyrins

The characteristic IR absorption spectral peaks data of the ruthenium porphyrins are listed in Table 2, and typical spectra are shown in Figures 6 (**2a**), 9 (**2b**), 12 (**2c**), 15 (**3a**), 18 (**3b**) and 21 (**4a**), which are consistent with literature records. The spectra show a strong and sharp absorption band around 1000 cm^{-1} which is assigned as the rocking vibration of the porphyrin ring or the pyrrole units.[3] Since this band is sensitivity to the ruthenium oxidation state, it is referred to as the "oxidation state marker".[3] For the carbonyl ruthenium(II) complexes (**2a-b**) (Figures 6, 9), the oxidation state marker band lies in the range of 1009 — 1012 cm^{-1}, and that for the *trans*-dioxoruthenium(VI) complexes (**3a-b**) (Figures 15, 18) are in the range of 1018 — 1022 cm^{-1}. Also, for dichlororuthenium complexes [Ru^{IV}(Cl)$_2$TMP](**4a**), the oxidation state marker band is around 1009 cm^{-1}.

The symmetric O=Ru=O stretches for all the *trans*-dioxoruthenium(VI) complexes (**3a-b**) show an distinct band at 822 cm^{-1} for **3a** and at 827 cm^{-1} for **3b**. The absence of the CO stretch indicates the starting carbonyl complexes have been completely consumed.[3]

Table 2. Selected IR Absorption Peaks of Ruthenium Porphyrin Complexes

Compound	Peak position / cm^{-1}		
	Oxidation marker band $V_{(pyrrolic\ C-H)}$	$V_{C=O}$	$V_{as(O=Ru=O)}$
2a	1009	1944	
2b	1012	1963	
2c	1011	1937	
3a	1018		822
3b	1022		827

3.5.4. ^{1}H-NMR Spectra of the Ruthenium Porphyrins

The free porphyrins (**1a**), and ruthenium porphyrins including [Ru^{II}(CO)(Por*)]

(**2a-2b**), [Ru^{VI}(O)$_2$(Por*)] (**3a-3b**) and Ru^{IV}(Cl)$_2$TMP (**4a**) complexes were also well

characterized by distinct ^{1}H-NMR spectra. Free porphyrin ligand (**1a**) was characterized

by the inner protons giving signals at $\delta \sim$ -2.5 ppm. Other than paramagnetic

Ru^{IV}(Cl)$_2$TMP (**4a**), others are consistent with a diamagnetic electronic ground state, d^6

for ruthenium(II) and d^2 for ruthenium(VI) complexes, respectively.[3] According to the

literature reports, the signals of the pyrrolic protons are known to be sensitive to the

electron density of the porphyrin which is in turn affected by the ruthenium oxidation

state.[3] The ^{1}H-NMR spectrum of the Ru^{IV}(Cl)$_2$TMP (**4a**) appears paramagnetically

shifted pyrrolic protons at δ -55.8 ppm in CDCl$_3$ in agreement with those reported.[20] For

ruthenium carbonyl complex **2a** (Figure 7), the pyrrolic protons show doublets peak

observed at 8.45 — 8.71 ppm. The ^{1}H-NMR spectrum of the *trans*-dioxoruthenium

complexes (**3a-b**) (Figure 16, 19) show the singlet of the pyrrolic protons at 8.79 and 9.18

ppm, which is downfield from that of the carbonyl ruthenium complexes. The change of

the multiplicity in the conversion from **2a** to **3a** is because the oxidation process is a

symmetry ascending process.[3] The characteristic ^{1}H-NMR spectrum chemical shifts

(ppm) data of the ruthenium porphyrins are listed in Table 3.

Table 3. ^{1}H Chemical Shifts (ppm) of the Ruthenium Porphyrin Complexes in CDCl$_3$

Compound	Chemical shifts, δ ppm			
	Pyrrolic H	Phenyl H	Methyl H	Inner H
1a	s, 8.61	s, 7.26	s, 1.81 (*o*)	s, -2.51
			s, 2.62 (*p*)	
2a	d, 8.45	s, 7.24	s, 1.84 (*o*)	
			s, 2.60 (*p*)	
2b	d, 8.71			
3a	s, 8.79	s, 7.23	s, 1.89 (*o*)	
			s, 2.62 (*p*)	
3b	s, 9.18			
4a	s, -55.8			
5a	s, -31.8			

IV. KINETIC STUDIES OF SULFOXIDATION BY *TRANS*-DIOXORUTHENIUM(VI) PORPHYRINS

4.1. Sulfoxidation Reactions

Organic ligand-complexes transition metal-oxo intermediates have been proposed as the active oxidizing species in many metal-catalyzed oxidation reactions that employ sacrificial oxidants such as hydrogen peroxide, peroxy acids, and iodosobenzene.[1,2] In this regard, *trans*-dioxoruthenium(VI) porphyrin complexes have been developed as the well-characterized model system to mimic heme-containing enzymes.[4] This class of compounds is reactive toward useful organic oxidations including alkene epoxidation and sulfoxidation as shown in Scheme 14.

Ar = 2,4,6-Me₃C₆H₂, TMP;
Ar = C₆H₅, TPP;
Ar = C₆F₅, TPFPP;
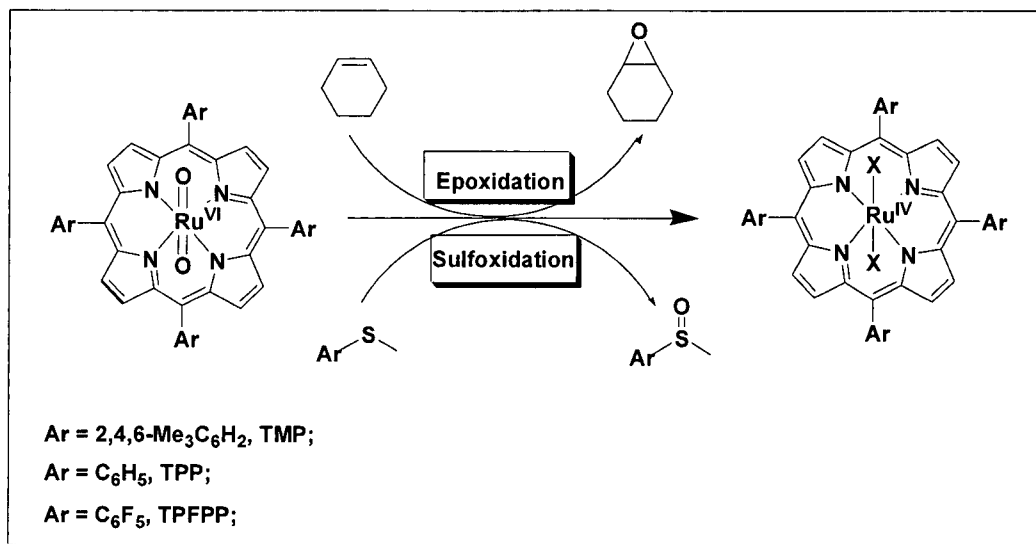
Scheme 14. Oxidation reactions by *trans*-dioxoruthenium(VI) porphyrin complexes

Kinetic studies of sulfoxidation and epoxidation reactions by the dioxoruthenium(VI) porphyrin complexes were performed as described in Section 2.4. The solution containing the *trans*-dioxoruthenium(VI) complexes was mixed with

solution containing large excesses of substrate, and pseudo-first-order rate constants were measured spectroscopically. The pseudo-first order rate constants, k_{obs} , were determined by monitoring the disappearance of the Soret band (λ_{max}= 422 nm for **3a** and λ_{max}= 413 nm for **3b**) of the *trans*-dioxoruthenium(VI) porphyrins in chloroform. Figure 26 showed the time-resolved UV-vis spectral change for the sulfide oxidation by the *trans*-dioxoruthenium(VI) porphyrin complex (**3a**) in chloroform. There were no intermediates accumulated during the whole process in view of the several obvious isosbestic points that could be observed during the change from Ru^{VI} to Ru^{IV} porphyrins. For $Ru^{VI}(O)_2TMP$ (**3a**), the decay of the Soret band of the *trans*-dioxoruthenium(VI) complex at 422 nm (λ_{max}) was accompanied by the formation of a new absorption at 407 nm (λ_{max}), which was blue-shifted in the sulfoxidation kinetics. For $Ru^{VI}(O)_2TPFPP$ (**3b**), the similar sulfoxidation process underwent red-shift-transformation from 412 nm to 420 nm. The typical time-resolved spectral were shown in Figure 26 (a-b).
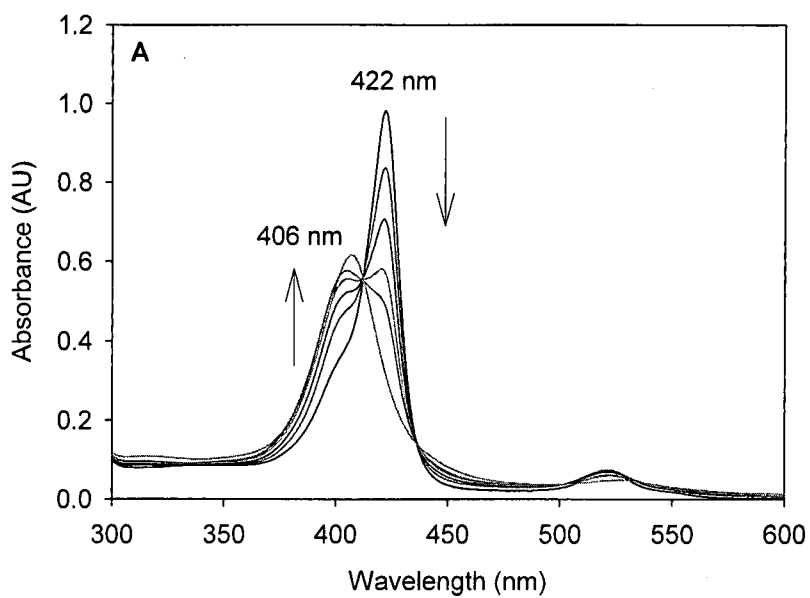
Figure 26. (a) Time-resolved spectrum for the reaction of **3a** with *p*-chlorothioanisole

(1mM) in CHCl₃ over 600 seconds.
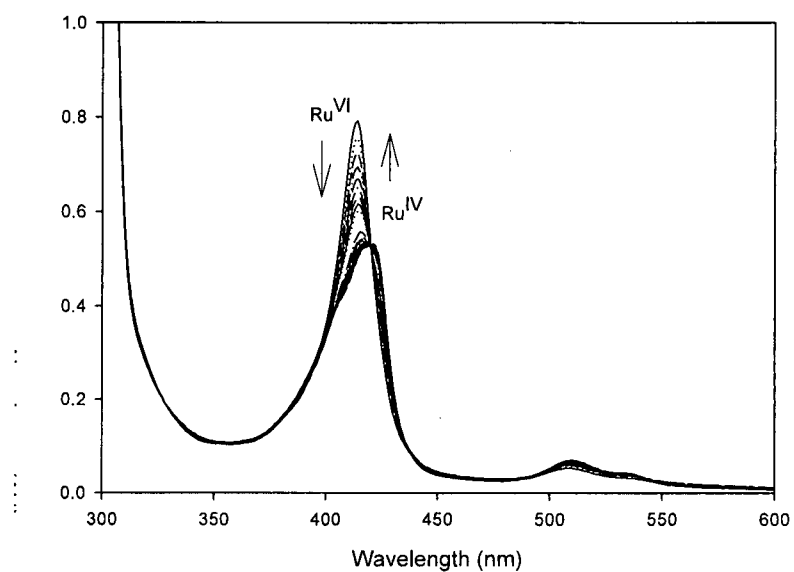
Figure 26. (b) Time-resolved spectrum for the reaction of **3b** with phenyl methyl sulfide

(0.125 mM) in CHCl₃ over 400 seconds.

As shown in the Figure 27, the kinetic traces were obtained at four different concentrations of sulfides during the process of sulfoxidation reactions. The rate of fast decay was directly proportional to the concentration of the substrates, i.e., the higher concentration of substrate gave the higher the rate of decay of complex.
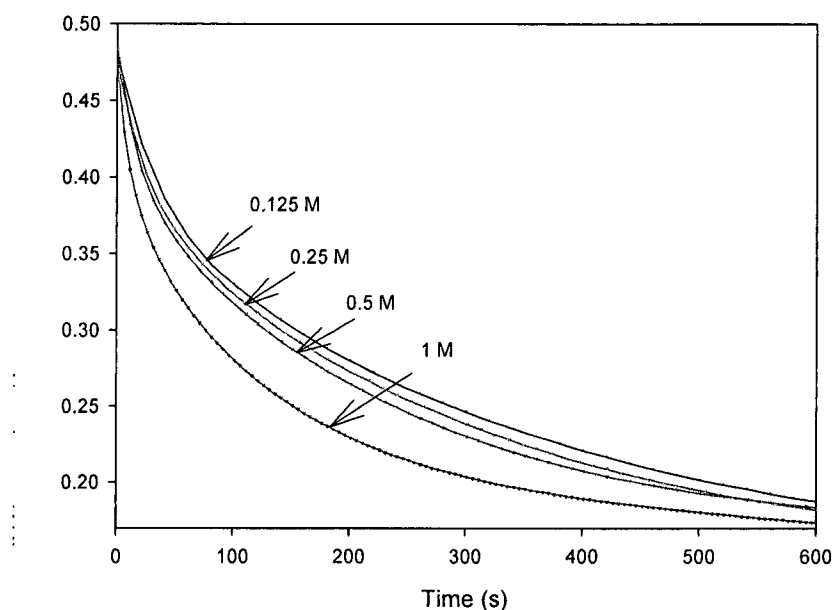
Figure 27. Kinetic traces monitored at 422 nm for the reaction of **3a** with *p*-chlorothioanisole at varied concentrations in CHCl₃.

Figure 28 showed a linear plot of observed pseudo-first-order rate constants (k_{obs}) versus the concentration of substrate. As described in Section 2.4, k_{obs} is the observed rate constant, k_0 is a background rate constant found in the absence of added substrate, k_2 is the second-order rate constant for reaction with the substrate and [Sub] is the molar concentration of the substrate. In a plot of k_{obs} versus the concentration of substrate, the slope was the second-order rate constant (k_2). The second-order rate constants for

reactions of *trans*-dioxoruthenium(VI) porphyrin complexes were summarized in Table 4. It is significant to note that the secondary reactions of sulfoxide oxidation to sulfone were not important under those conditions since the concentration of substrates were several orders of magnitude larger than the concentrations of products formed in the reactions. As shown in Figure 29, the effect of substituent on substrates for sulfoxidation reactions with **3b** was minor, indicting no appreciable charge developed at the sulfur during the oxidation process.

Table 4. Second-Order Rate Constants (k_2) for the Reactions of a Variety of Substrates by Ruthenium Porphyrin Complexes in $CHCl_3$ at $22 \pm 2^{\circ}C$.

Metal-oxo Species	Substrate	k_2 ($M^{-1}s^{-1}$)
[Ru^{VI}(O)$_2$TMP]	thioanisole	8.00 ± 0.4
3a	*p*-fluorothioanisole	3.00 ± 0.3
	p-chlorothioanisole	8.10 ± 0.5
[Ru^{VI}(O)$_2$TPP]	thioanisole	48.0 ± 2.0
[Ru^{VI}(O)$_2$TPFPP]	thioanisole	59.6 ± 2.0
3b	*p*-fluorothioanisole	56.0 ± 1.0
	p-chlorothioanisole	42.4 ± 3.0
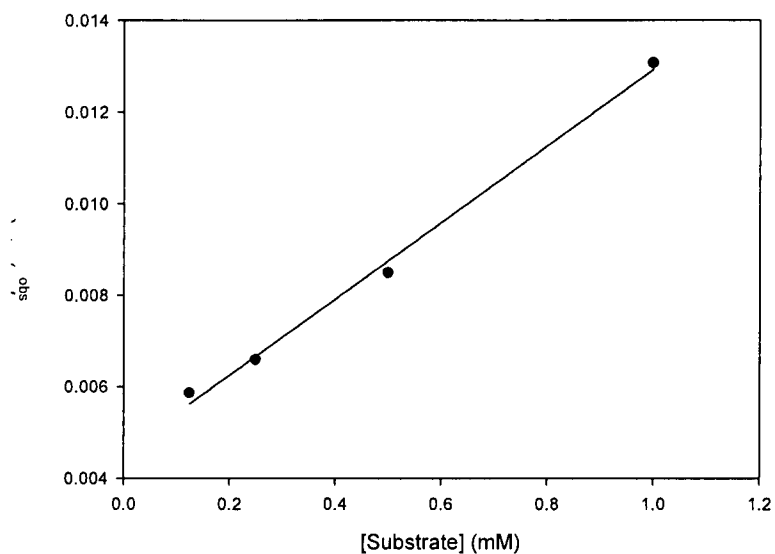
Figure 28. The kinetic plot of the reaction of **3a** with *p*-chlorothioanisole at the concentrations of 1 mM, 0.5 mM, 0.25 mM and 0.125 mM.
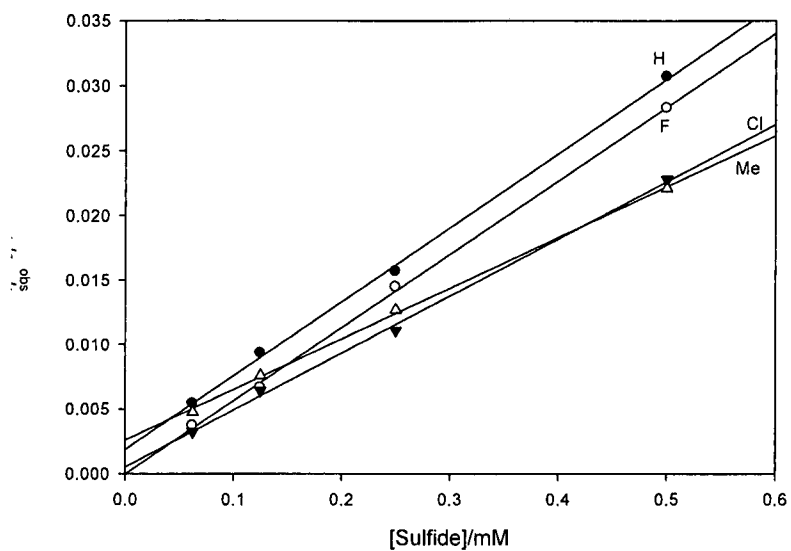
Figure 29. Observed rate constants for the reaction of **3b** with different substrates; thioanisole (H), *p*-fluorothioanisole (F), *p*-chlorothioanisole (Cl), and *p*-methylthioanisole (Me).

For comparison, the well-known epoxidation of cycloalkenes by the dioxo complexes was also studied under identical conditions. In the past decades, the kinetic studies of epoxidation of alkenes by *trans*-dioxoruthenium(VI) porphyrin complexes have been well documented.[36] Following the similar procedure, the time-resolved spectrum and kinetic plot of epoxidation reactions of **3a** with styrene were obtained as shown in Figures 30 and 31.
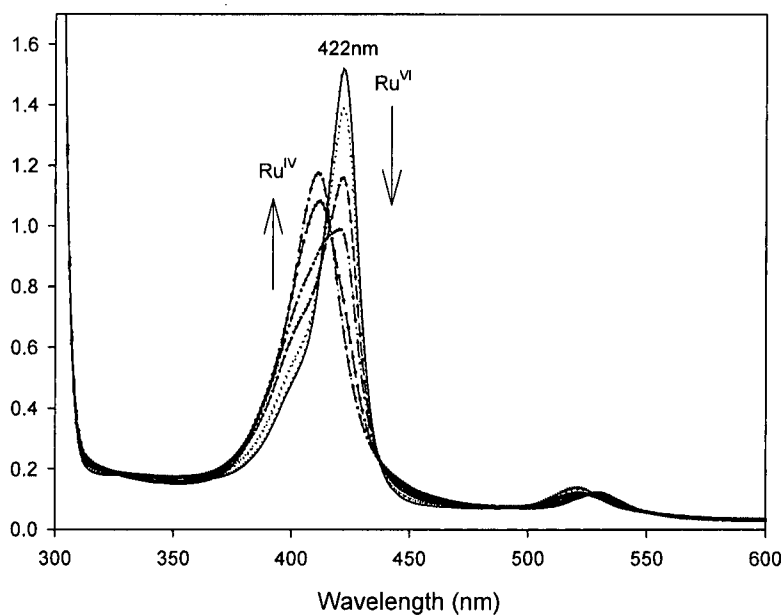
Figure 30. Time-result spectra of the reaction of **3a** with 0.5 M styrene in $CHCl_3$ over 600s.
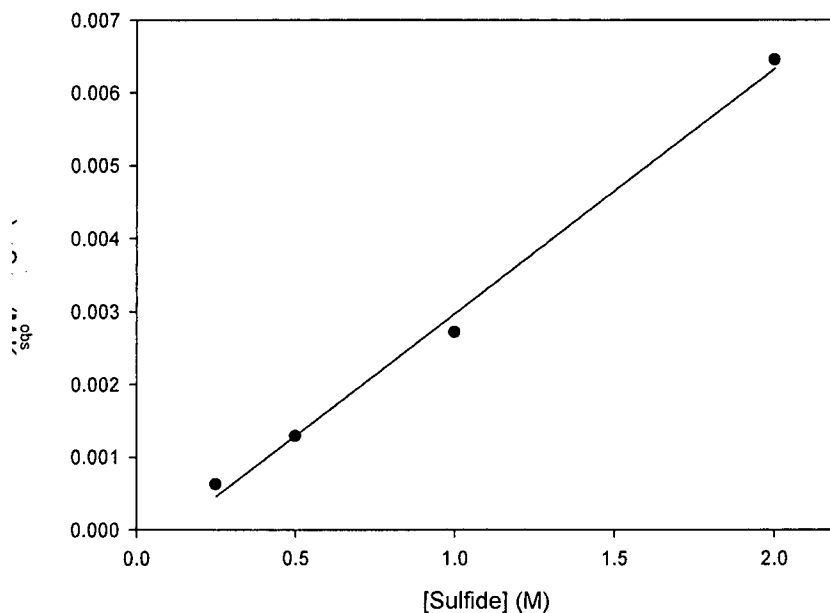
Figure 31. Kinetic plot of the reactions of **3a** with styrene at 2 M, 1 M, 0.5 M and 0.25 M.

Similar to sulfoxidation reactions, the transformation showed the decay of the Soret band of the *trans*-dioxoruthenium(VI) complex at 422 nm (λ_{max}) accompanied by the formation of a new absorption[3] at 407 nm (λ_{max}). The observed isosbestic points also indicated that there were no intermediates accumulated during the epoxidation process. In Figure 31, the kinetic plot is linear as function of substrate concentrations. The second-order rate constant (k_2) of 4.4 x 10^{-3} $M^{-1}s^{-1}$ was solved from the slope of the kinetic plot. The kinetic comparison clearly showed the sulfoxidation reactions are 3 to 4 orders of magnitude faster than the epoxidation reactions.

In Table 4, the sulfoxidation kinetic data of *trans*-dioxo-(5, 10, 15, 20-tetraphenylporphyrinato) ruthenium(VI) [$Ru^{VI}(O)_2TPP$] were also included for comparison. With the obtained kinetic results, the reactivity order of *trans*-

dioxoruthenium(VI) complex followed $Ru^{VI}(O)_2TPFPP > Ru^{VI}(O)_2TPP > Ru^{VI}(O)_2TMP$.

As shown in Table 4, the significant difference among the reactivities of different *trans--*

dioxoruthenium(VI) porphyrin complexes by reacting with thioanisole indicted the trend

of reactivities of ruthenium-oxo porphyrins. Noticeably, the oxidation reaction of

thioanisole by **3b** gave the highest second-order rate constant k_2 of 59.6 $M^{-1}s^{-1}$, which

revealed **3b** was the most reactive. There were 20 fluorine atoms on the aryl groups of

porphyrin ligand that significantly increased the electrophilicity of **3b**. According to the

report by Che et al.,[38] halogenations on porphyrin ligand made the reactive metal-oxo

intermediate more electron demanding by reducing the electron density of the porphyrin

ring, thus promoting its reactivity and the catalyst stability toward oxidations. Complex

$Ru^{VI}(O)_2TMP$ (**3a**) is the least reactive due to the steric effect of 12 methyl substitutes on

aryl groups of the porphyrin. Thus, the methyl groups induced a fence around Ru = O,

and blocked the access of organic substrates to metal center.
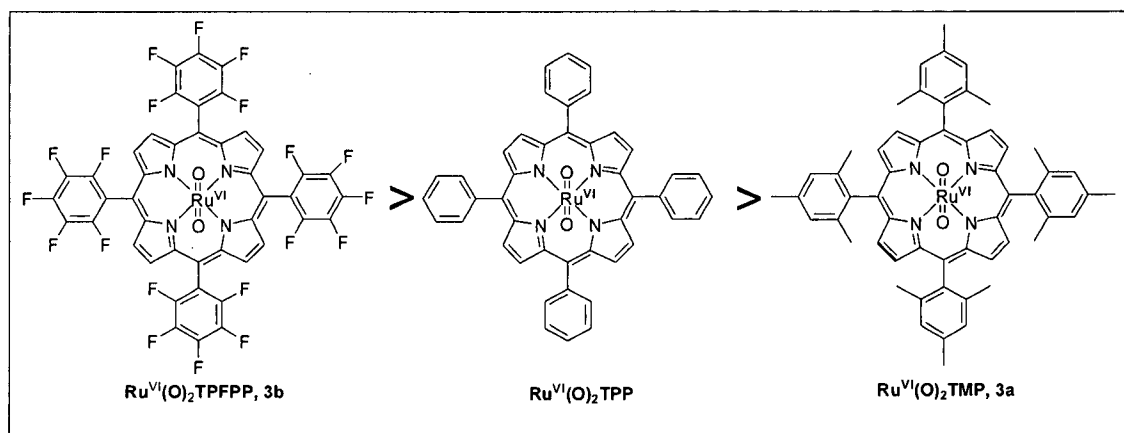
Scheme 15. Reactivity order of the *trans*-dioxoruthenium(VI) porphyrin complexes in

sulfoxidation reactions.

4.2. Competition Studies of Sulfoxidation Reactions

One objective of this study is to identify the oxidants during catalytic turnover conditions with transition metal catalysts.[41] Identifying the kinetically competent oxidants in catalytic reactions could lead to better control of the catalytic oxidation reactions, especially in terms of selectivities. There was one method to evaluate whether the same species was active in the two sets of conditions by comparing the ratios of products formed under catalytic turnover conditions to the ratios of rate constants measured in the direct kinetic studies. If the same oxidant was present in both cases, the ratios of absolute rate constants from direct measurements and relative rate constants from the competition studies should be similar, although a coincident similarity for two different oxidants could not be excluded. When the ratios were not similar, however, the active oxidants under the two sets of conditions must be different.[41] To this end, the competitive sulfoxidation reactions catalyzed by carbonyl ruthenium(II) porphyrin complexes with different sacrificial oxidants were conducted as described in Section 2.5.

Table 5 contains the results of kinetic results with *trans*-dioxoruthenium(VI) porphyrin complexes and competition reactions where PhIO and TBHP were employed as sacrificial oxidants with carbonyl ruthenium(II) porphyrin catalysts, respectively. In this study, a limiting amount of sacrificial oxidant was used to keep the conversion less than 20%. The amounts of substrates consumed were determined, as opposed to the amounts of oxidation products formed; this method reduced potential problems in product analysis due to secondary oxidations and multiple oxidation products.[42]

Table 5. Relative Rate Constants for Porphyrin-Ruthenium-Oxo Reactions[a]

Porphyrin	Substrates	Oxidant	k_{rel}[b]
TPFPP	thioanisole/p-fluorothioanisole	kinetic results	1.06
		PhIO	0.83
		TBHP	0.69
TPFPP	thioanisole/p-chlorothioanisole	kinetic results	1.41
		PhIO	0.82
		TBHP	0.50
TPFPP	thioanisole/p-methylthioanisole	kinetic results	1.51
		PhIO	1.02
		TBHP	1.50
TPFPP	thioanisole/p-methoxythioanisole	kinetic results	1.57
		PhIO	1.31
TMP	thioanisole/p-chlorothioanisole	kinetic results	0.99
		PhIO	0.59
		TBHP	0.83

[a] A reaction solution containing equal amounts of two substrates, e.g., thioanisole (0.5 mmol) and substituted thioanisole (0.5 mmol), ruthenium(II) porphyrin catalyst (1 μmol) and an internal standard of 1,2,4-trichlorobenzene (0.5 mmol) was prepared in CH_3Cl (5 mL). Iodosobenzene (PhIO) or *tert*-butly hydroperoxide (TBHP) (0.2 mmol) was added, and the mixture was stirred overnight (22h) under an inert atmosphere at 23 ± 2 °C. The amounts of substrates before and after the reactions were determined by GC analysis with DB-5 capillary column. [b] Relative ratios of absolute rate constants from kinetic results with *trans*-dioxoruthenium(VI) porphyrin complexes and for competitive oxidations with various carbonyl ruthenium(II) porphyrin catalysts at ambient temperature.

Comparing the selectivity (k_{rel}) found in competitive oxidation reactions (one oxidant presented with two reductants) to the ratio of absolute rate constants found in

direct kinetic studies of the same reductants, the oxidants during catalytic turnover conditions with carbonyl ruthenium(II) porphyrin complexes could be deduced. For example, the ratio of absolute rate constants for kinetic reaction of **2b** with thioanisole/ *p*-methylthioanisole was similar to the ratio of products found in competitive catalytic oxidations oxidized by *tert*-butyl hydroperoxide. For most of the cases where the absolute rate constants for oxidation reactions of the two substrates differed substantially, the ratio of rate constants was consistently smaller than the ratio of absolute rate constants. Although the differences appear to be small, they were statistically significant, which implied the *trans*-dioxoruthenium(VI) porphyrins were unlikely to be the sole active oxidant under turnover conditions, and also suggested that the *trans*-dioxoruthenium(VI) porphyrins were less reactive (higher selectivity) than the species formed in the catalytic reactions.
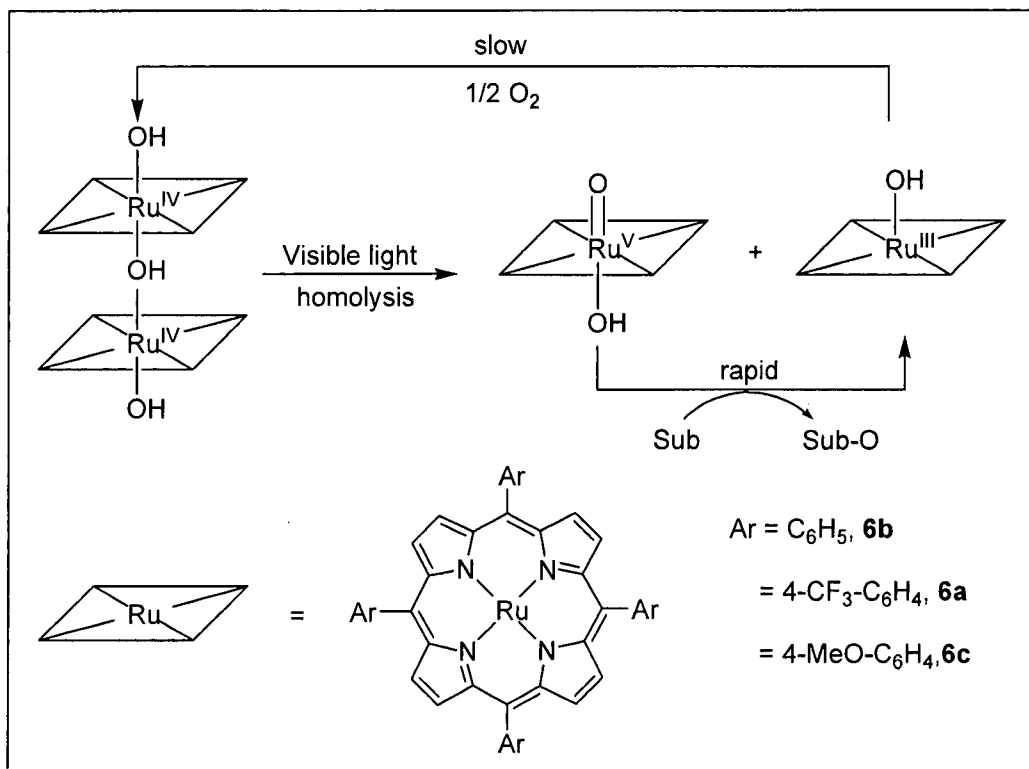
V. PHOTOCATALYTIC AEROBIC OXIDATION BY A BIS-PORPHYRIN-RUTHENIUM(IV) μ-OXO DIMER

5.1. <u>Introduction</u>

Selective oxidation is a significant technology for the synthesis of high value chemicals in the pharmaceutical and petrochemical industries, but the oxidations are among the most problematic processes to control.[1] Many stoichiometric oxidants with heavy metals are expensive and/ or toxic and impractical. The ideal green catalytic oxidation process would use atmospheric oxygen as the primary oxygen source, recyclable catalysts in nontoxic solvents and an inexpensive energy source. In this work, the photochemical generation of highly reactive metal-oxo intermediates for useful catalytic oxidation was investigated.[26]

Among the high-valent metal-oxo species, metal(V)-oxo complexes deserve special attention because they are highly reactive, although rare and elusive. According to report by Zhang and co-workers, the known porphyrin manganese(V)-oxo complexes showed higher reactivity than well-studied iron(IV)-oxo porphyrin radical cation analogues.[42] Furthermore, the porphyrin-ruthenium(V)-oxo transients are attractive candidates for oxidations, and these species are proposed intermediates in very efficient catalytic processes,[32] although not yet observed directly. In this study, the photocatalytic aerobic oxidation of hydrocarbons by the ruthenium(IV) μ-oxo bisporphyrin complexes using visible light and atmospheric oxygen as oxygen source was investigated. As shown in Scheme 16, the catalytic sequences were proposed via a photodisproportionation

pathway to give a putative ruthenium(V)-oxo species serving as the actual oxidizing agent.

Scheme 16. Photocatalytic aerobic oxidation by a bis-porphyrin-ruthenium(IV) μ-oxo dimer.

5.2. Synthesis and Characterization of Bis-Porphyrin-Ruthenium(IV) μ-Oxo Dimers

According to the known method described by Sugimoto and co-workers[43], the bis-porphyrin-ruthenium(IV) μ-oxo dimer **6a** was synthesized by the following procedure (Scheme 17). $Ru^{II}(CO)(4-CF_3-TPP)$ (50 mg) was placed in a 100 mL round-bottom flask with 70% aqueous *tert*-butyl hydroperoxide (0.5 mL) and benzene (50 mL). The reaction mixture was stirred at room temperature until the color of the solution turned from orange

red to dark brown. After removal of the benzene under reduced pressure, the residual

solid was chromatographed on an alumina with dichloromethane as an eluant. The

binuclear ruthenium(IV) complex obtained in this study showed diamagnetic spectra in

^{1}H-NMR spectra. The alternative interpretation of the diamagnetism— a through space

coupling of the macrocycles under an ruthenium (IV) porphyrin radical formalism— was

not supported by the structure, since it would require a smaller separation of the two

porphyrins and a more parallel orientation. The desired dimer bis-porphyrin-

ruthenium(IV) μ-oxo dimer [Ru^{IV}(4-CF$_3$-TPP)(OH)]$_2$O (6a) was characterized by UV-vis

(Figure 32) and ^{1}H-NMR (Figure 33), consistent with the literature reported.[43]
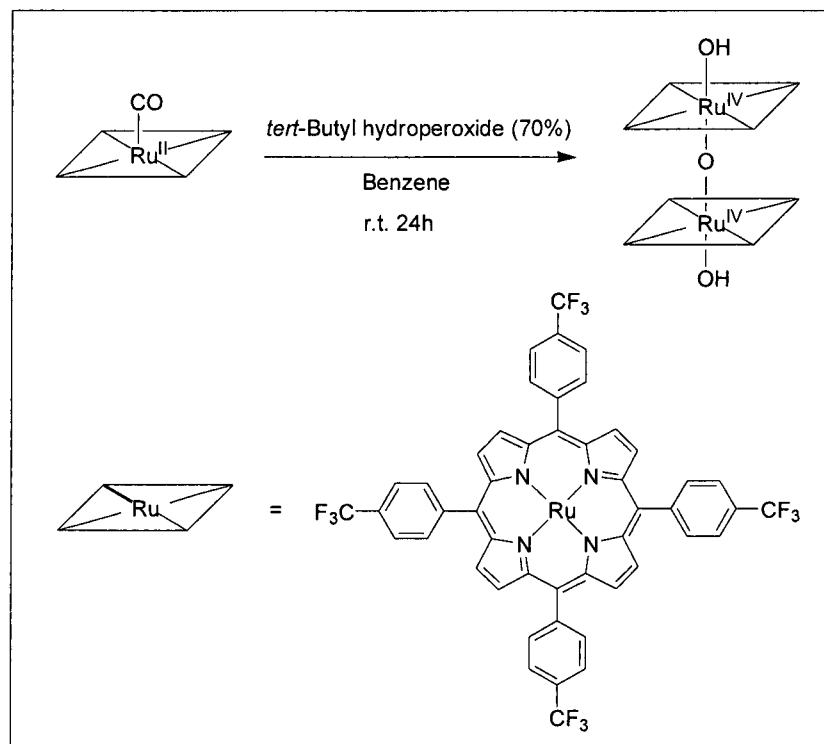
Scheme 17. Synthesis of [Ru^{IV}(4-CF$_3$-TPP)(OH)]$_2$O (6a)
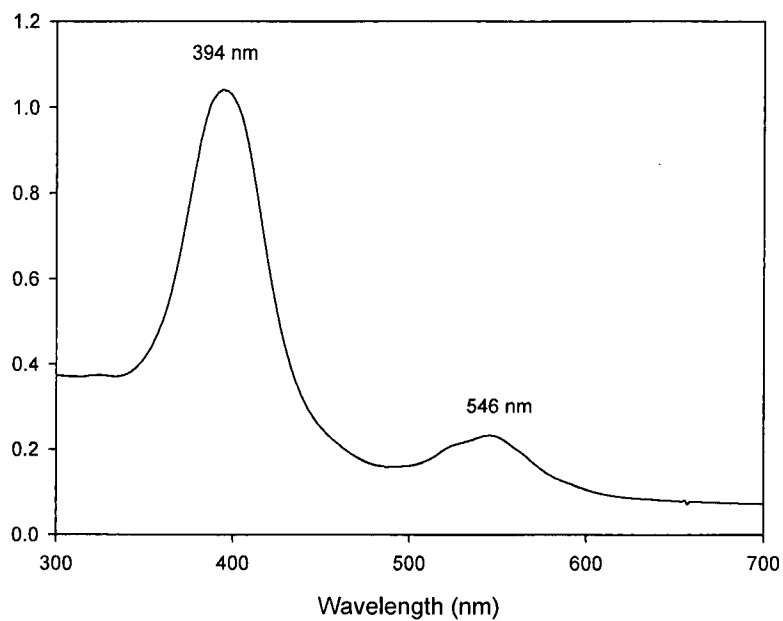
Figure 32. The UV-vis spectrum of [Ru^{IV}(4-CF$_3$-TPP)(OH)]$_2$O (**6a**) in CHCl$_3$.
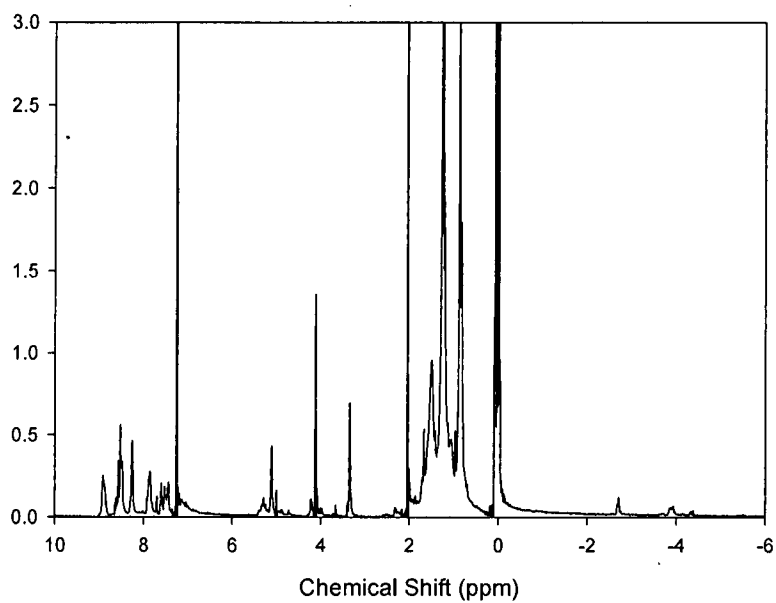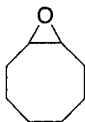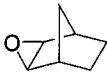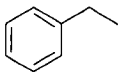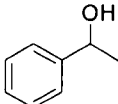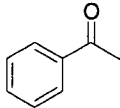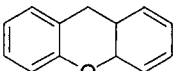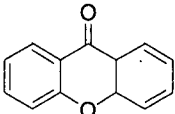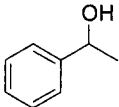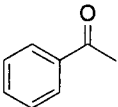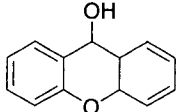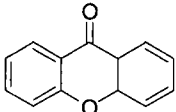
Figure 33. The ^{1}H-NMR spectrum of [Ru^{IV}(4-CF$_3$-TPP)(OH)]$_2$O (**6a**) in CDCl$_3$.

5.3. Photocatalytic Aerobic Oxidation by a Bis-Porphyrin-Ruthenium(IV) μ-Oxo Dimer (6a)

The ruthenium(IV) μ-oxo bisporphyrin **6a** was evaluated in the aerobic oxidation of a variety of organic substrates. The reactions were carried out as described in Section 2.6. Table 6 listed the oxidized products and corresponding turnovers using **6a** as the photocatalyst.

As shown in Table 6, the trend in the TONs roughly paralleled the substrate reactivity, and significant activity was observed with up to 3900 TON. After 24 hours photolysis, *cis*-cyclooctene and norbornene were oxidized to the corresponding epoxides with 200 ~ 250 TONs (entries 1 and 2). Activated hydrocarbons including ethylbenzene and xanthenes were oxidized to the corresponding alcohols and/or ketones from overoxidation with total TONs 560 and 2900, respectively (entries 3 and 4). It was noticeable that the oxidation of secondary benzylic alcohols gave the highest catalytic activities (entries 5and 6). For comparison, the photocatalytic aerobic epoxidation of *cis*-cyclooctene by the well-known $Ru^{VI}(O)_2TMP$ (**3a**) was also conducted under the identical condition. Only 30 TON was obtained (data was not shown). Obviously, the $[Ru^{IV}(4\text{-}CF_3\text{-}TPP)(OH)]_2O$ (**6a**) was much more efficient photocatalyst than the well-known $Ru^{VI}(O)_2TMP$ (**3a**).

Table 6. Turnover Numbers for Alkenes and Benzylic C-H Oxidations Using $[Ru^{IV}(4\text{-}CF_3\text{-}TPP)(OH)]_2O$ (**6a**) as the Photocatalyst.[a]

Entry	Substrate	Product	TON
1	cis-cyclooctene	cis-1,2-epoxycyclooctane	250 ± 21
2	norbornene	norbornene oxide	200 ± 40
3	ethylbenzene	1-phenylethanol	380 ± 41
		acetophenone	180 ± 19
4	xanthene	9-xanthone	2900 ± 140
5	1-phenylethanol	acetophenone	3300 ± 240
6	9-xanthenol	9-xanthone	3900 ± 280

[a] The reactions were typically carried out with 0.5 mg of catalyst in the 10 mL oxygen-saturated solution containing 2 ~ 4 mmol of substrates. In most cases, 5 ~ 10 mg of anthracene was added to enhance the

catalytic activity. After 24 hours of photolysis with visible light (λ_{max} = 420 nm), a known amount of 1,2,4-trichlorobenzene was added as an internal standard for GC analysis. [b] Determined for a 24 h photolysis (λ_{max} = 420 nm). The values reported are the average of 2~ 3 runs.

Competitive catalytic oxidation of ethylbenzene and ethylbenzene-d_{10} revealed a kinetic isotope effect (KIE) of k_H/k_D = 4.8 ± 0.2 at 298K, which was larger than those observed in autoxidation processes, suggesting a nonradical mechanism that involved the intermediacy of ruthenium(V)-oxo species as postulated in Scheme 16. The observed photocatalytic oxidation is ascribed to a photodisproportionation mechanism to afford a putative porphyrin-ruthenium(V)-oxo species that can be directly observed and kinetically studied by laser flash photolysis methods. Further studies to characterize the observed transients more fully and to define synthetic applications are ongoing in our laboratory.

VI. CONCLUSION

The *trans*-dioxoruthenium(VI) porphyrins have been among the best-characterized metal-oxo intermediates and their involvement as the active oxidant in the alkene epoxidations and alkane hydroxylation have been extensively studied. Following the literature known methods, a series of ruthenium porphyrin complexes have been synthesized and spectroscopically characterized. The *trans*-dioxoruthenium(VI) porphyrin complexes (**3a-b**) were synthesized from the oxidation of the corresponding carbonyl ruthenium(II) porphyrin precursors with *m*-CPBA. All the spectroscopical data including UV-vis, IR, and ^{1}H-NMR are consistent with literature values. In addition, a new preparation of *trans*-dioxoruthenium(VI) porphyrin complexes was developed by an extremely easy photochemical approach, and the generality of the methodology was demonstrated in sterically encumbered and unencumbered systems under same conditions.

The kinetics of two-electron oxidations of *para*-substituted phenyl methyl sulfides by *trans*-dioxoruthenium(VI) porphyrin complexes was studied using stopped-flow spectroscopy. The decay of *trans*-dioxoruthenium(VI) porphyrins in the presence of reactive sulfides follows a biexponential process with pseudo-first order kinetics to form Ru(IV) species. The reactivity order in the series of dioxo complexes follows TPFPP>TPP>TMP, consistent with expectations based on the electrophilic nature of high-valent metal-oxo species. For comparison, the sulfoxidation reactions are 3 to 4 orders of magnitude faster than the well-known epoxidation reactions. It was found that the effect of substituent on substrate for the oxidation of *para*-substituted thioanisoles was minor, suggesting no appreciable charge developed at the sulfur during the oxidation process. In addition, ruthenium porphyrins were used as the catalysts in the competitive

71

oxidation reactions to identify the kinetically competent oxidants during catalytic turnover conditions. The ratios of rate constants for oxidations by **3** were larger than the observed product ratios from competition studies, suggesting that dioxoruthenium(VI) complexes (**3**) were less reactive than the oxidizing species formed in catalytic reactions.

The photocatalytic aerobic oxidation of hydrocarbons by the ruthenium(IV) μ-oxo bisporphyrin complexes using visible light and atmospheric oxygen as oxygen source was investigated. The ruthenium(IV) μ-oxo bisporphyrin **6a** was found to catalyze aerobic oxidation of a variety of organic substrates efficiently. Significant activity was observed with TONs up to 3900. For comparison, the photocatalytic aerobic epoxidation of *cis*-cyclooctene by **3a** was also conducted under the identical condition. Obviously, **6a** was more efficient photocatalyst than the well-known **3a**. Competitive catalytic oxidation of ethylbenzene and ethylbenzene-d_{10} revealed a larger KIE value at 298K than those observed in autoxidation processes, suggesting a nonradical mechanism that involved the intermediacy of ruthenium(V)-oxo species as postulated.

REFERENCES

1. Backwell, J.-E.; Piera J. "Catalytic oxidation of organic substrates by molecular oxygen and hydrogen peroxide by multistep electron transfer – A biomimetic approach." *Angew. Chem. Int. Ed.* **2008**, *47*, 3506 – 3523.

2. Brink, G.-J.; Arends, I.W.C.E.; Sheldon, R.A. "Green catalytic oxidation of alcohols in water." *Science*, **2000**, *287*, 1636 – 1639.

3. Zhang, R. "Asymmetric organic oxidation by chiral ruthenium complexes containing D_2- and D_4- symmetric porphyrinato ligands." *Ph. D. Thesis* **2000**, 1 – 235.

4. Denisov, L.-G.; Makris, M.-T.; Sligar, G.-S.; Schlichting, L. "Structure and chemistry of cytochrome P450." *Chem. Rev.* **2005**, *105*, 2253 – 2277.

5. Masanori, S.; Roach, M.-P.; Coulter, E.-D.; Dawson, J.-H. "Heme-containing oxygenases." *Chem. Rev.* **1996**, *96*, 2841 – 2887.

6. Hamilton, G.A. *In molecular mechanisms of oxygen activation*; Hayaishi, O., Ed.; Academic: New York, 1974; Chapter 10, 405 – 451.

7. Meunier, B. *Metal-oxo and metal-peroxo species in catalytic oxidations*. Academic Press: New York, 2000.

8. Ullrich, V. *Topics in current chemistry*. 1979, 83: 67.

9. Zhang, R.; Nagraj, N.; Lansakara-P.,D.S.P.; Hager, L.-P.; Newcomb, M. "Kinetics of two-electron oxidation by the Compound I derivative of

chloroperoxidase, a model for cytochrome P450 oxidants." *Org. Lett.* **2006**, *8*, 2731 – 2734.

10. Groves, J.-T. "Reactivity and mechanism of metalloporphyrin-catalyzed oxidations." *J. Porph. Phthal.* **2000**, *4*, 350 – 352.

11. Sheldon, R, Kochi J. *Metal-catalyzed oxidations of organic compounds.* Academic Press: New York, 1981.

12. Simandi, L. *Dioxygen activation and homogeneous catalytic oxidation.* Elsevier: Amsterdam, 1991.

13. Wang, C.; Shalyaev, K.V.; Bonchio, M.; Carofiglio, T.; Groves, J.T. "Fast catalytic hydroxylation of hydrocarbons with ruthenium porphyrins." *Inorg. Chem.* **2006**, *45*, 4769 – 4782.

14. Meunier B. "Metalloporphyrins as versatile catalysts for oxidation reactions and oxidative DNA cleavage." *Chem. Rev.* **1992**, *92*, 1411 – 1456.

15. Davies, J. *Selective hydrocarbon activation: Principle and progress.* VCH: New York, 1994.

16. Ortiz de Montellano, P.R. (Ed.), *Cytochrome P450 structure, mechanism, and biochemistry*, 2nd Ed., Plenum, New York, 1995.

17. Dey, A.; Ghosh, A. "Ture iron(V) and iron(VI) porphyrins: a first theoretical exploration." *J. Am. Chem. Soc.* **2002**, *124*, 3206 – 3207.

18. Collins, T.; Oliveira, F.; Chanda, A.; Banerjee, D.; Shan, X.; Mondal, S. "Chemical and Spectroscopic Evidence for an Fe^V-Oxo Complex." *Science*. **2007**, *315*, 835 – 838.

19. Groves, J.T.; Lee, J.; Marla, S.S. "Detection and characterization of an oxomanganese(V) porphyrin complex by rapid-mixing stopped-flow spectrophotometry." *J. Am. Chem. Soc.*, **1997**, *119*, 6269 – 6273.

20. Huang, Y.; Vanover, E.; Zhang, R. "A facile photosynthesis of *trans*-dioxoruthenium(VI) porphyrins." *Chem. Commun.*, **2010**, *46*, 3776 – 3778.

21. Kowalski, P.; Mitka, K.; Ossowska, K.; Kolarska, Z. "Oxidation of sulfides to sulfoxides. Part1: Oxidation using halogens derivatives." *Tetrahedron* **2005**, *61*, 1933 – 1953.

22. Surendra, K.; Krishnaveni, N.S.; Kumar, V.P.; Sridhar, R.; Rao, K.R. "Selective and efficient oxidation of sulfides to sulfoxides with *N*-bromosuccinimide in the presence of *β*-cyclodextrin in water." *Tetrahedron Lett.* **2005**, *46*, 4581 – 4583.

23. Nehlsen, J.P.; Benziger, J.B.; Kevrekidis, I.G. "Removal of alkanethiols from a hydrocarbon mixture by a heterogeneous reaction with metel oxides." *Ind. Eng. Chem. Res.* **2003**, *42*, 6919 – 6923.

24. Golchoubian, H.; Hosseinpoor, F. "Mn(III)-catalyzed oxidation of sulfides to sulfoxides with hydrogen peroxide." *Tetrahedron Lett.* **2006**, *47*, 5195 – 5197.

25. Chellamani, A; Alhaji, N.M.I.; Rajagopal, S. "Kinetics and mechanism of (salen)MnIII – catalyzed hydrogen peroxide oxidation of alkyl aryl sulphides." *J. Phys. Org. Chem.* **2007**, *20*, 255 – 263.

26. Vanover, E.; Huang, Y.; Xu, L.-B.; Newcomb, M.; Zhang, R. "Photocatalytic aerobic oxidation by a bis-porphyrin-ruthenium(VI) μ-oxo dimer: observation of a putative porphyrin-ruthenium(V)-oxo intermediate." *Org. Lett.* **2010**, *12*, 2246 – 2249.

27. Gross, Z.; Mahammed, A.; Gray,H.; Meier-Callahan, A. "Aerobic Oxidations Catalyzed by Chromium Corroles." *J. Am. Chem. Soc.* **2003**, *125*, 1162 – 1163.

28. Bäckvall, J. E. *Modern oxidation methods*; Wiley-VCH Verlag: Wemheim, 2004.

29. Punniyamurthy, T.; Velusamy, S.; Iqbal, J. "Recent advances in transition metal catalyzed oxidation of organic substrates with molecular oxygen." *Chem. Rev.*, **2005**, *105*, 2329 – 2364.

30. Peterson, M.W.; Rivers, D.S.; Richman, R.M. "Mechanistic considerations in the photodisproportionation of μ-oxo-bis((tetraphenylporphinato)iron(III))." *J. Am. Chem. Soc.*, **1985**, *107*, 2907–2915.

31. Rosenthal, J.; Pistorio, B.J.; Chng, L.L. "Aerobic catalytic photooxidation of olefins by an electron-deficient pacman bisiron(III) μ-oxo porphyrin." *J. Org. Chem.* **2005**, *70*, 1885 – 1888.

32. Groves, J.T.; Bonchio, M.; Carofiglio, T.; Shalyaev, K. "Rapid catalytic oxygenation of hydrocarbons by ruthenium pentafluorophenylporphyrin complexes: evidence for the involvement of a Ru(III) intermediate." *J. Am. Chem. Soc.* **1996,** *118,* 8961-8962.

33. Che, C.-M.; Huang, J.-S. "Metalloporphyrin-based oxidation systems: From biomimetic reactions to application in organic synthesis." *Chem. Commun.* **2009,** *55,* 3996-4015.

34. Lindsey, J.S.; Wagner, R.W. "Investigation of the synthesis of *ortho*-substituted tetraphenylporphyrins." *J. Org. Chem.* **1989,** *54,* 828 – 836.

35. Leung, W.H.; Che, C.M. "High-valent ruthenium(IV) and – (VI) oxo complexes of octaethylporphyrin. Synthesis, spectroscopy, and reactivities." *J. Am. Chem. Soc.* **1989,** *111,* 8812 – 8818.

36. Che, C.-M.; Zhang, J.-L.; Zhang, R.; Huang, J.-S.; Lai, T.-S.; Tsui, W.-M, Zhou, X.-G.; Zhou, Z.-Y.; Zhu, N.; Chang, C.K. "Hydrocarbon oxidation by β-halogenated dioxoruthenium(VI) porphyrin complexes: Effect of reduction potential (RuVI/V) and C – H bond-dissociation energy on rate constants." *Chem. Eur. J.* **2005,** *11,* 7040 – 7053.

37. Hartmann, M.; Robert, A.; Duarte, V.; Keppler, K.B.; Meunier, B. "Synthesis of water-soluble ruthenium porphyrins as DNA cleavers and potential cytotoxic agents." *J. Biol. Inorg. Chem.*, **1997,** *2,* 427 – 432.

38. Groves, J.T.; Quinn, R. "Models of oxidized heme proteins. Preparation and characterization of a *trans*-dioxoruthenium(VI) porphyrin complex." *Inorg. Chem.* **1984**, *23*, 3844 – 3846.

39. Gross, Z.; Barzilay, C.M. "A novel facile synthesis of dihalogenoruthenium(IV) porphyrins." *J. Chem. Soc., Chem. Commun.*, **1995**, 1287 – 1288.

40. Ho, C.L.; Leung, W.-H.; Che, C.M. "Kinetics of C – H bond and alkene oxidation by *trans*-dioxoruthenium(VI) porphyrins." *J. Chem. Soc., Dalton Trans.*, **1991**, 2933-2939.

41. Zhang, R.; Newcomb, M. "Laser flash photolysis generation of high-valent transition metal-oxo species: Insights from kinetic studies in real time." *Acc. chem. Res.*, **2008**, *41*, 468 – 477.

42. Pan, Z.-Z.; Zhang, R.; Newcomb, M. "Kinetic studies of reactions of iron(IV)-oxo porphyrin radical cations with organic reductants." *J. Inorg. Biochem.* **2006**, *100*, 524 – 532.

43. Sugimoto, H.; Higashi, T.; Mori, M.; Nagano, M.; Yoshida, Z.-I.; Ogoshi, H. "Preparation and physicochemical properties of new linear μ-oxo bridged ruthenium(IV) and osmium(IV) porphyrin dimers." *Bull. Chem. Soc. Jpn.* **1982**, *55*, 822 – 828.

PUBLICATIONS AND PRESENTATIONS

(A) Articles in peer-reviewed journals

1. **Huang, Y.**; Vanover, E.; Zhang, R. A facile photosynthesis of *trans*-dioxoruthenium(VI) porphyrins. *Chem. Commun.*, **2010**, *46*, 3776 – 3778.

2. Vanover, E.; **Huang, Y.**; Xu, L-B.; Newcomb, M.; Zhang, R. Photocatalytic aerobic oxidation by a bis-porphyrin-ruthenium(VI) μ-oxo dimer: observation of a putative porphyrin-ruthenium(V)-oxo intermediate. *Org. Lett.* **2010**, *12* (10), 2246–2249.

(B) Presentations at academic conferences

1. Abebrese, C.; **Huang, Y.**; Cartwright, W.; Zhang, R. (2008) : Kinetics of Oxidation of Aryl Methyl Sulfides by *trans*-Dioxoruthenium(VI) Porphyrin Complexes, 60th SERMACS, American Chemical Society, Nashville, TN, November 2008.

2. Cartwright, W.; Abebrese, C.; **Huang, Y.**; Zhang, R. (2008) : Generation and Kinetic Studies of High-Valent Metal-Oxo species: Implication for Cytochrome P450 Oxidants, 94th Kentucky Academy of Science Annual Meeting, Lexington, KY, November 2008.

3. **Huang, Y.**; Abebrese, C.; Zhang, R. (2009) : Kinetics of Oxidation of Aryl Methyl Sulfides by *trans*-Dioxoruthenium(IV) Porphyrin Complexes, WKU Student Research Conference, Bowling Green, KY, February 2009.

4. Cartwright, W.; Abebrese, C.; **Huang, Y.**; Zhang, R. (2009) : Generation and kinetic studies of high-valent ruthenium-oxo porphyrin intermediates. 237th Annual American Chemical Society Meeting, Salt Lake City, UT, March 2009.